Removal of Artifacts from Electrocardiogram

Thesis submitted in partial fulfilment of the requirements for the degree

of

Master of Technology

in

Electronics and Communication Engineering

(Specialization: Electronics and Instrumentation)

by

Rashmi Panda

Roll No: 210EC3185

Department of Electronics & Communication Engineering

National Institute of Technology Rourkela

Rourkela, Odisha-769008

May 2012

Removal of Artifacts from Electrocardiogram

Thesis submitted in partial fulfilment of the requirements for the degree

of

Master of Technology

in

Electronics and Communication Engineering

(Specialization: Electronics and Instrumentation)

by

Rashmi Panda

Roll No: 210EC3185

Under the Supervision of

Dr. Umesh Chandra Pati

Department of Electronics & Communication Engineering

National Institute of Technology Rourkela

Rourkela, Odisha-769008

May 2012

Dedicated

to

My parents

Department of Electronics and Communication Engineering
National Institute of Technology Rourkela
Rourkela - 769008, Odisha, India.

Certificate

This is to certify that the work in the thesis entitled **"Removal of Artifacts from Electrocardiogram"** by **Rashmi Panda** is a record of an original research work carried out by her under my supervision and guidance in partial fulfilment of the requirements for the award of the degree of Master of Technology with specialization in *Electronics and Instrumentation* from the department of *Electronics and Communication Engineering*, National Institute of Technology Rourkela. Neither this thesis nor any part of it has been submitted for any degree or academic award elsewhere.

Date:

Dr. Umesh Chandra Pati
Associate Professor
Dept. of Electronics and Comm. Engg.
National Institute of Technology
Rourkela-769008

Acknowledgement

The real spirit of achieving a goal is through the way of excellence and austere discipline. I would have never succeeded in completing my task without the cooperation, encouragement and help provided to me by various personalities.

I am grateful to numerous local and global peers who have contributed towards shaping this thesis. At the outset, I would like to express my sincere thanks to Dr. Umesh Chandra Pati for his advice during my thesis work. As my supervisor, he has constantly encouraged me to remain focused on achieving my goal. His observations and comments helped me to establish the overall direction of the research and to move forward with investigation in depth. He has helped me greatly and been a source of knowledge.

I am also thankful to all the professors of the department for their support and encouragement.

I must acknowledge the academic resources that I have got from NIT Rourkela. I would like to thank administrative and technical staff members of the Department who have been kind enough to advise and help in their respective roles.

I am really thankful to my all friends. My sincere thanks to everyone who has provided me with kind words, a welcome ear, new ideas, useful criticism, or their invaluable time, I am truly indebted.

I would conclude with my deepest gratitude to my parents, my husband and all my loved ones. My full dedication to the work would have not been possible without their blessings and moral support. This thesis is a dedication to them who did not forget to keep me in their hearts when I could not be beside them.

Rashmi Panda

rashmipanda1986@gmail.com

Abstract

The electrocardiogram is the recording of the electrical potential of heart versus time. The analysis of ECG signal has great importance in the detection of cardiac abnormalities. The electrocardiographic signals are often contaminated by noise from diverse sources. Noises that commonly disturb the basic electrocardiogram are power line interference, instrumentation noise, external electromagnetic field interference, noise due to random body movements and respirational movements. These noises can be classified according to their frequency content. It is essential to reduce these disturbances in ECG signal to improve accuracy and reliability.

Different types of adaptive and non-adaptive digital filters have been proposed to remove these noises. In this thesis, window based FIR filters, adaptive filters and wavelet filter bank are applied to remove the noises. Performances of the filters are compared based on the PSNR values. It is difficult to apply filters with fixed filter coefficients to reduce the instrumentation noise, because the time varying behaviour of this noise is not exactly known. Adaptive filter technique is required to overcome this problem, as the filter coefficients can be varied to track the dynamic variations of the signals. In wavelet transform, a signal is analyzed and expressed as a linear combination of the summation of the product of the wavelet coefficients and mother wavelet. The wavelet decomposition offers an excellent resolution both in time and frequency domain. Better estimation of the amplitudes is also obtained in wavelet based denoising.

Keywords: ECG denoising, FIR filter, adaptive filter, wavelet decomposition, PSNR

Contents

List of figures .... **viii**

List of tables .... **x**

List of abbreviations .... **xi**

Chapter 1

Introduction **1**

1.1 Introduction 2

1.2 Literature survey 3

1.3 Objective of the thesis 4

1.4 Thesis organization 5

Chapter 2

Basics of ECG and Artifacts **6**

2.1 Electrocardiogram 7

2.1.1 Structure and physiology of heart 7

2.2 Generation of heart beat 9

2.3 ECG morphology 10

2.4 Noises in ECG 12

2.4.1 Power line interference 12

2.4.2 Electrode contact noise 13

2.4.3 Motion artifacts 13

2.4.4 Electromyographic noise 13

2.4.5 Instrumentation noise 14

2.5 ECG database 14

Chapter 3

ECG Denoising Algorithms **16**

3.1 FIR filtering 17

3.1.1 Design techniques of FIR filters 17

3.1.2 The window based FIR filter design 18
3.2 Adaptive filtering 21
3.2.1 Adaptive algorithms 22
3.3 Wavelet denoising 24
3.3.1 Wavelet Transform 24
3.3.2 Discrete Wavelet Transform 25
3.3.3 Wavelet Decomposition 27
3.3.4 Wavelet reconstruction 28
3.3.5 ECG denoising using wavelet transform 29

Chapter 4

Results and Discussion 31
4.1 ECG waveform 32
4.2 Generation of noises 32
4.2.1 Generation of low frequency noise (base line wander) 32
4.2.2 Generation of high frequency noise 33
4.2.3 Generation of power line interference 34
4.3 Addition of noises to ECG 34
4.4 Results of window based FIR filtering 35
4.5 Results of adaptive filtering 37
4.6 Results of wavelet filter bank based denoising 40

Chapter 5

Conclusion and Future Scope 45
5.1 Conclusion 46
5.2 Future scope 47

Bibliography 48

Dissemination 53

List of figures

Figure 2.1 Structure of heart 8
Figure 2.2 Conduction path of electrical potential for heart beat 9
Figure 2.3 ECG waveform 10
Figure 3.1 Adaptive filter structure 21
Figure 3.2 Single stage wavelet filtering 27
Figure 3.3 Single stage wavelet filtering with down sampling 27
Figure 3.4 Multistage wavelet decomposition tree 28
Figure 3.5 single stage decomposition and reconstruction 29
Figure 4.1 ECG Signal from MITBIH arrhythmia database 32
Figure 4.2 a)sine wave of frequency 0.1 Hz b)sine wave of frequency 0.02 Hz c)triangular wave of frequency 0.05 Hz d) Base linewander........ 33
Figure 4.3 High frequency noise 33
Figure 4.4 Power line interference 34
Figure 4.5 Corrupted ECG signal 34
Figure 4.6 ECG signal after passing through FIR filter with Rectangular Window 35
Figure 4.7 ECG signal after passing through FIR filter with Hamming window 35
Figure 4.8 ECG signal after passing through FIR filter with Hanning window 36
Figure 4.9 ECG signal after passing through FIR filter with Blackman window 36
Figure 4.10 (a) ECG signal after passing through LMS based filter (b) Error plot after passing through LMS based adaptive filter 37
Figure 4.11 (a) ECG signal after passing through NLMS based filter (b) Error plot after passing through NLMS based adaptive filter 38
Figure 4.12 (a) ECG signal after passing through SDLMS based filter (b) Error plot after passing through SDLMS based adaptive filter 38
Figure 4.13 (a) ECG signal after passing through SELMS based filter (b) Error plot after passing through SELMS based adaptive filter 39
Figure4.14 (a) ECG signal after passing through S**S**LMS based filter (b) Error plot after passing through S**S**LMS based adaptive filter........ 39

Figure 4.15 Noisy ECG signal used in wavelet filter bank based denoising 40
Figure 4.16 Symlet scaling function φ 41
Figure 4.17 Symlet wavelet function ψ 41
Figure 4.18 Approximation coefficients a) cA_1: approximation coefficients at level 1, b)cA_2: approximation coefficients at level 2, c)cA_3 : approximation coefficients at level 3, d) cA_4 : approximation coefficients at level 42
Figure 4.19 Detailed coefficients a) cD_1 : detailed coefficients at level 1, b) cD_2:detailed coefficients at level 2,c)cD_3: detailed coefficients at level 3,d)cD_4: detailed coefficients at level 4 43
Figure 4.20 Approximated noise 44
Figure 4.21 Denoised ECG using wavelet filter bank 44

List of tables

Table 2.1 Features of ECG signal 11
Table 4.1 PSNR comparison of window based FIR filters 37
Table 4.2 PSNR values of various adaptive filters 40

List of abbreviations

ECG	Electrocardiogram
MIT-BIH	Massachusetts Institute of Technology Beth Israel Hospital database
SA node	Sinoatrial node
AV node	Atrioventricular node
ANS	Autonomic Nervous system
SNS	Sympathetic Nervous System
PNS	Parasympathetic Nervous System
FIR	Finite Impulse Response
IIR	Infinite Impulse Response
LMS	Least Mean Square
NLMS	Normalized Least Mean Square
SDLMS	Sign-Data Least Mean Square
SELMS	Sign-Error Least Mean Square
SSLMS	Sign-Sign Least Mean Square
WT	Wavelet Transform
CWT	Continuous Wavelet Transform
DWT	Discrete Wavelet Transform
IDWT	Inverse Discrete Wavelet Transform
LPF	Low Pass Filter
HPF	High Pass Filter

Chapter 1

Introduction

Literature survey

Objective of the thesis

Thesis organization

This chapter is the preface to rest of the thesis. This comprises of a brief introduction to ECG denoising followed by literature survey which includes all the important contributions to the field of ECG enhancement. The rest part of this chapter contains objective of the thesis and thesis organization.

1.1 INTRODUCTION

Electrocardiogram (ECG) is the record of the electrical potentials produced by the heart. The electrical wave is generated by depolarization and repolarization of certain cells due to movement of Na+ and k^+ ions in the blood. The ECG signal is typically in the range of 2 mV and requires a recording bandwidth of 0.1 to 120 Hz [1]. The ECG is acquired by a non-invasive technique, i.e. placing electrodes at standardised locations on the skin of the patient [2]. The ECG signal and heart rate reflects the cardiac health of human heart. Any disorder in heart rate or rhythm or change in the morphological pattern of ECG signal is an indication of cardiac arrhythmia. It is detected and diagnosed by analysis of the recorded ECG waveform. The amplitude and duration of the P-QRS-T-U wave contains useful information about the nature of disease related to heart.

In clinical environment during acquisition, the ECG signal encounters various types of artifacts. The ones of primary interest are power line interference, external electromagnetic field interference, noise due to random body movements and respirational movements, electrode contact noise, electromyography (EMG) noise, and instrumentation noise. These noises degrade the signal quality, frequency resolution and strongly affect the morphology of ECG signal containing important information. It is essential to reduce disturbances in ECG signal and improve the accuracy and reliability for better diagnosis.

Many methods have been implemented to remove the noise from noisy ECG signal. The basic method is to pass the signal through high pass, low pass and notch filters. But these filters are examples of static filters. One of the biggest disadvantages of this static filter is that these also remove some important frequency components in the vicinity of cut off frequency. The static filters have fixed filter coefficients. It is difficult to reduce the instrumentation noise with fixed filter coefficients, because the time varying behaviour of this noise is not exactly known. To overcome the limitations of static filters, different adaptive filtering methods have been developed. Other examples of dynamic filters are adaptive Kalman filter, wiener filter, modified extended Kalman filter etc. ECG denoising is also done by wavelet based filters an neural networks. In this thesis, various filters have been implemented for reduction of noise in ECG. Their performances are also compared based on the PSNR values.

1.2 LITERATURE SURVEY

During past few years, various contributions have been made in literature regarding noise removal, beat detection and classification of ECG signal. Most of them use either time or frequency domain representation of the ECG waveforms.

In the paper, "Application of the digital filter for noise reduction in electrocardiogram", S.K. Jagtap , M.S. Chavan, R.C. Wagvekar and M.D. Uplane have implemented high pass, low pass window based FIR filters using Rectangular, Hamming, Hanning, Kaiser windows for noise reduction in electrocardiogram [3]. The order of filter is taken as 100. They have analysed the performance by comparing signal power before and after filtration. With this order, the FIR filter with rectangular window has sharp attenuation and pulsation present in the stop band and pass band. The phase response of rectangular was linear and the filter was found to be stable, in comparison to others.

In 2010, Dr. K.L. Yadav and S. Singh have used adaptive algorithms i.e. LMS and RLS for noise cancellation in their paper "Performance evaluation of different adaptive filters for ECG signal processing" [4]. According to their paper, the RLS algorithm based adaptive filter has better performance.

In the paper "Efficient sign based normalised adaptive filtering techniques for cancellation of artefacts in ECG signals: Application to wireless biotelemetry", M.Z. Rahman, R.A. Shaik and D.V. Rama Koti Reddy have used several simple and efficient sign based normalized adaptive filters for cancelation of noise in electrocardiographic (ECG) signals, which are computationally superior having multiplier free weight update loops [5]. The proposed implementation is suitable for applications such as biotelemetry, where large signal to noise ratios with less computational complexity are required.

C.H. Chang, K.M. Chang and H.J. Ko have compared the adaptive algorithm performance for noise cancellation with and without using the external reference in their paper "Cancellation of high-frequency noise in ECG signals using Adaptive filter without external reference" [6]. The adaptive filter with reference is often ineffective due to the fact that the reference signal cannot be well correlated with the noise part in the primary input. Therefore, the adaptive filter without external reference was implemented.

Over the past several years, methods based on the wavelet transform (WT) have also received a great deal of attention for the denoising of signals that possess multiresolution characteristics such as the ECG [7]–[12].

In the paper titled, “Optimal selection of wavelet basis function applied to ECG signal denoising”, B. N. Singh and A. K. Tiwari have applied an optimal wavelet basis function for denoising of an ECG signal [13]. The experimental results have revealed suitability of Daubechies mother wavelet of order 8 to be the most appropriate wavelet basis function for the denoising application.

Several other techniques have been also proposed to extract the ECG components contaminated with the background noise and allow the measurement of subtle features in the ECG signal. Statistical techniques such as principal component analysis [14], independent component analysis [15], [16], and neural networks [17] have also been used to extract a noise free signal from the noisy ECG.

1.3 OBJECTIVE OF THE THESIS

The condition of heart is generally reflected in the nature of ECG waveform and heart rate. ECG, if properly analyzed, can provide important information regarding various disorders and diseases related to heart. However, ECG being a non-stationary signal, the irregularities are not periodic and do not show up all the time, but is noticeable at certain irregular intervals during the day. Hence, clinical observation of ECG takes long hours and it is very tedious. Moreover, visual analysis can not be relied upon as the possibility of the analyst missing the vital information is high. Sometimes the important informations are lost due to various types of artifacts. Hence, computer based analysis and denoising of ECG signal are done before diseases diagnosis.

The most difficult problem faced in automatic ECG analysis is the large variation in the morphologies of ECG waveforms. Moreover, we have to consider the time constraints as well.

Thus, the basic objective of the thesis is to come up with a simple algorithm to remove artifacts having less computational complexity without compromising with the efficiency. This objective has motivated me to search and experiment with various techniques for noise reduction in ECG.

1.4 THESIS ORGANIZATION

The thesis constitutes five chapters including this chapter. The rest of the thesis is organized as follows:

Chapter 2: Basics of ECG and Artifacts

This Chapter explains the generation of heart beat, basics of electrocardiogram and ECG morphology. Artifacts that commonly appear in ECG signal during acquisition are elaborately discussed. Different modes of lead placement and the MIT-BIH arrhythmias database are also described.

Chapter 3: ECG Denoising Algorithms

This chapter discusses different approaches which are implemented in this thesis to denoise the ECG signal. Different window based FIR filtering approach, adaptive filters, wavelet filter bank technique are explained in this chapter.

Chapter 4: Results and Discussion

In this chapter, the ECG signals taken from MIT-BIH database and noises generated according to their frequency content are shown. Then, the noisy ECG signal (ECG + noise generated) are passed through the designed filters. This chapter presents all the results of the filters discussed in chapter-3 under separate subsections. The Performance analyses of all these filters are also done on the basis of their PSNR values.

Chapter 5: Conclusions and Future Work

This chapter presents analytical remarks to overall achievements and limitations of all the proposed works and scope for further research work in this domain.

Chapter 2

Basics of ECG and Artifacts

Structure and physiology of heart

Generation of heartbeat

ECG morphology

Noises in ECG

ECG database

This Chapter explains basics of electrocardiogram, the generation of heart beat and morphology of ECG waveform. Artifacts that commonly appear in ECG signal during acquisition are elaborately discussed. Different modes of lead placement and the MIT-BIH arrhythmia database are also described.

2.1 ELECTROCARDIOGRAM

The ECG is a bioelectric signal, which records the electrical activity of heart versus time. Therefore, it is an important diagnostic tool for assessing heart function [18]. The ECG is acquired by placing electrodes on the skin of the patient. The ECG signal provides the following information of a human heart [19]:

- disturbances in heart rhythm and conduction
- abnormalities in the spread of electrical impulse across the heart
- information about a prior heart attack
- sign of coronary artery disease
- abnormal thickening of heart muscle
- indication of decreased oxygen delivery to the heart
- extent and location of myocardial ischemia
- changes in electrolyte concentrations
- effects of drugs on the heart

2.1.1 Structure and Physiology of Heart

The human heart weighs 250- 350 grams and is approximately equal to the size of the fist. It is located anterior to the vertebral column and posterior to the sternum. It is covered by a double-walled sac called the pericardium. The exterior part of this sac is called the fibrous pericardium. This sac protects the heart, anchors its surrounding structures and prevents overfilling of the heart with blood. The outer wall of the human heart is composed of three layers. The outer layer is called the epicardium or visceral pericardium since it is also the inner wall of the pericardium. The middle layer is called the myocardium and is composed of cardiac muscle which contracts. The inner layer is called the endocardium and is in contact with the blood. It also merges with the inner lining (endothelium) of blood vessels and covers heart valves [20].

The Heart is divided into separate right and left sections by the interventricular septum. Each of these (right and left) sections are again divided into upper and lower compartments known as atria and ventricles respectively. Thus, human heart has four chambers i.e. two superior atria and two inferior ventricles. The atria are the receiving chambers and the ventricles are the discharging chambers as shown in the Fig. 2.1. The atria are attached to the ventricles by fibrous, non-conductive tissue that keeps the ventricles electrically isolated from the atria. The Tricuspid valve separates the right atrium from the right ventricle. The Mitral (also known as the Bicuspid) valve separates the left atrium from the left ventricle.

Oxygen-poor blood from the whole body is received into the right atrium through large veins called the superior and inferior vena cava and flows. The right atrium and the right ventricle together form a pump to the circulate blood to the lungs [21]. The right ventricle then pumps the blood to the lungs where the blood is oxygenated. Similarly, the left atrium and the left ventricle together form a pump to circulate oxygen-enriched blood received from the lungs (via the pulmonary veins) to the rest of the body [22].

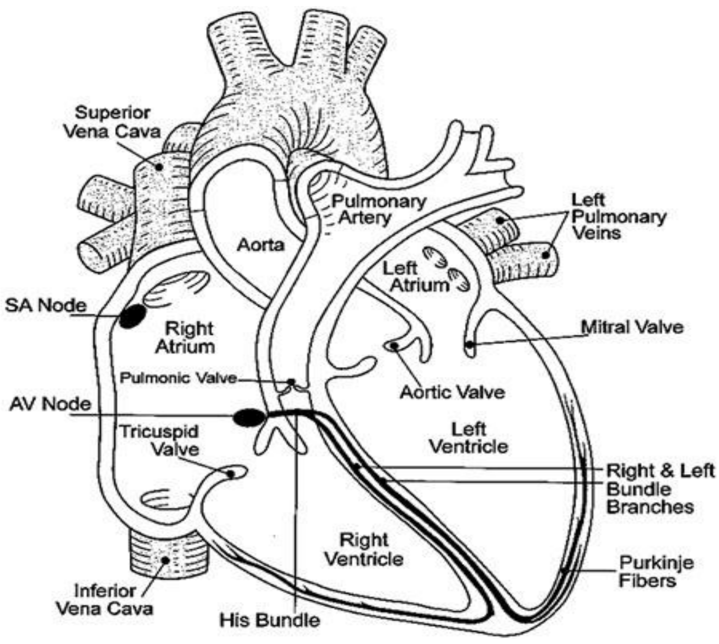

Figure 2.1 Structure of heart

2.2 GENERATION OF HEART BEAT

Some cardiac cells are self-excitable, contracting without any signal from the nervous system. Even if removed from the heart and placed in culture, the cells have the self-excitation property. The electrical potentials for contraction are caused by a group of specialized cells in the heart which control the heartbeat. These cells produce electrical impulses which spread across the heart causing it to contract. The main pacemaker of heart, the Sinoatrial node (SA node), initiates the heart beat by generating an electrical impulse which travels to the left and right atria, causing them to contract (atrial depolarization). Following the start of atrial depolarization, the impulse quickly arrives at the Atrioventricular node (AV node) which is responsible for the contraction of ventricle. The electrical signal next passes through the Bundle of His, diverges into the Right and Left Bundle branches, and spreads through the Purkinje Fibers to the muscles of the left and right ventricle. This causes ventricular depolarization (contraction). The time required for the signal to travel from the AV node to the Purkinje Fibers provides a natural delay of about 0.1 second. This delay ensures that the atria have become completely empty before the ventricles contract. The contraction is followed by ventricular repolarization (recovery) of the cells which were excited during the previous depolarization wave.

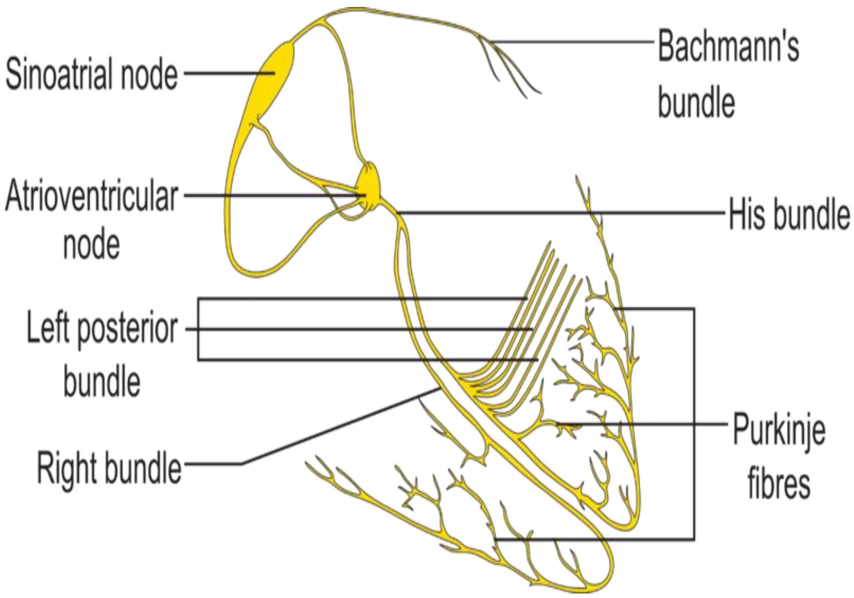

Figure 2.2 Conduction path of electrical potential for heart beat

The SA node creates the electrical impulse which causes the heart to beat, but the Autonomic Nervous System (ANS) controls the heart rate and the strength of heart contractions. The ANS consists of two parts, the Sympathetic Nervous System (SNS) and the Parasympathetic Nervous System (PNS). The Sympathetic nerves increase the heart rate and the contraction force, while the Parasympathetic nerves act in the reverse manner. An idealized conduction of electrical impulse for heart beat is shown in Fig. 2.2. A small portion of this electrical potential flows to the body surface. By applying electrodes on the skin at the selected points, the electrical potential generated by this current can be recorded as an ECG signal [23].

2.3 ECG MORPHOLOGY

ECG waveform of a normal individual consists of P wave, QRS complex, ST segment, T wave and U wave. The labels of Fig. 2.3 are commonly used in medical ECG terminology.

P wave: When the electrical impulse is conducted from the SA node towards the AV node and spreads from right to left atrium, the depolarization (contraction) of the atria occurs. The depolarization of atria results the P Wave in the ECG [20].

QRS complex: The QRS complex consists of three waves, sequentially known as Q, R and S. The rapid depolarization of both the ventricles results this complex. The muscles of the ventricles have large muscle mass than that of atria, hence its amplitude is much larger than that of P wave.

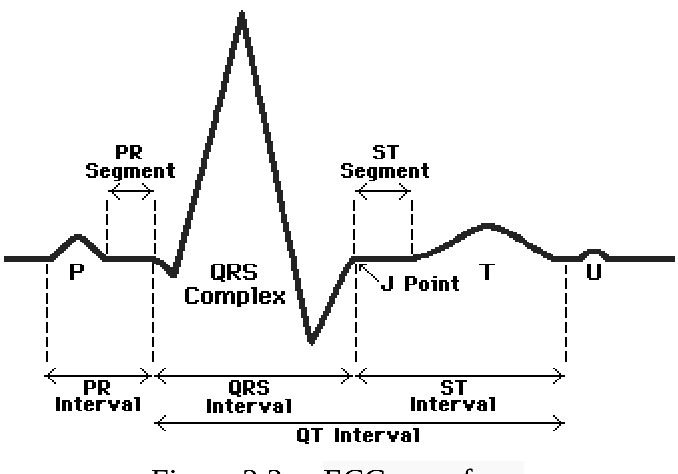

Figure 2.3 ECG waveform

T wave: Ventricular repolarisation results the preceding of ST segment and the T wave.

U wave: The origin of U wave is not clear and it is rarely seen. It is probably produced due to the repolarisation of the papillary muscles [23].

Table 2.1 shows different features of ECG along with the intervals and amplitudes.

Table 2.1 Features of ECG signal

Features	Description	Amplitude	Duration
P wave	Atrial depolarization	0.1-0.2 mv	80 ms
PR interval	Reflects the time the electrical impulse takes to travel from the sinus node through the AV node and entering the ventricles	_	120-200ms
QRS complex	Depolarization of ventricles	1-1.2 mv	80-120 ms
J point	Point where QRS complex is finished	_	_
ST interval	Represents the period when the ventricles are depolarized		80-120 ms
T wave	Repolarisation of ventricles	0.12-0.3mv	160 ms
QT interval	is measured from the beginning of the QRS complex to the end of the T wave. A prolonged QT interval is a risk factor for ventricular tachyarrhythmias and sudden death	_	300-430ms
U wave	repolarisation of the papillary muscles, rarely seen	_	_
RR interval	The interval between an R wave and the next R wave	_	0.2-1.2 s

2.4 NOISES IN ECG

ECG measurements may be corrupted by many sorts of noise. The ones of primary interest are:

- Power line interference
- Electrode contact noise
- Motion artifacts
- EMG noise
- Instrumentation noise

These artifacts strongly affects the ST segment, degrades the signal quality, frequency resolution, produces large amplitude signals in ECG that can resemble PQRST waveforms and masks tiny features that are important for clinical monitoring and diagnosis. Cancelation of these artifacts in ECG signals is an important task for better diagnosis.

2.4.1 Power Line Interference

Power line interference occurs through two mechanisms: capacitive and inductive coupling. Capacitive coupling refers to the transfer of energy between two circuits by means of a coupling capacitance present between the two circuits. The value of the coupling capacitance decreases with increasing separation of the circuits. Inductive coupling on the other hand is caused by mutual inductance between two conductors. When current flows through wires it produces a magnetic flux, which can induce a current in adjacent circuits. The geometry of the conductors as well as the separation between them determines the value of the mutual inductance, and hence the degree of the inductive coupling. Typically, capacitive coupling is responsible for high frequency noise while inductive coupling introduces low frequency noise. For this reason inductive coupling is the dominant mechanism of power line interference in electro cardiology. To limit the amount of power line interference, electrodes should be applied properly, that there are no loose wires, and all components have adequate shielding.

The Power line interference has frequency of 60 Hz or 50 Hz depending on the power supply.

2.4.2 Electrode Contact Noise

Electrode contact noise is caused by variations in the position of the heart with respect to the electrodes and changes in the propagation medium between the heart and the electrodes. This causes sudden changes in the amplitude of the ECG signal, as well as low frequency baseline shifts. In addition, poor conductivity between the electrodes and the skin reduces the amplitude of the ECG signal and increases the probability of disturbances (by reducing SNR).

The underlying mechanism resulting in these baseline disturbances is electrode-skin impedance variation. The larger the electrode-skin impedance, the smaller the relative impedance change needed to cause a major shift in the baseline of the ECG signal. If the skin impedance is extraordinarily high, it may be impossible to detect the signal features reliably in the presence of body movement. Sudden changes in the skin-electrode impedance induce sharp baseline transients which decay exponentially to the baseline value. This transition may occur only once or rapidly several times in succession. Characteristics of this noise signal include the amplitude of the initial transition and the time constant of the decay.

2.4.3 Motion Artifacts

Motion artifacts are baseline changes caused by electrode motion. The usual causes of motion artifacts are vibrations, movement, or respiration of the subject. The peak amplitude and duration of the artifacts are random variables which depend on the variety of unknowns such as the electrode properties, electrolyte properties (if one is used between the electrode and skin), skin impedance, and the movement of the patient. In this ECG signal, the baseline drift occurs at an unusually low frequency (approximately less than 1Hz).

2.4.4 Electromyographic Noise

Electromyographic noise is caused by the contraction of other muscles besides the heart. When other muscles in the vicinity of the electrodes contract, they generate depolarization and repolarisation waves that can also be picked up by the ECG. The extent of the crosstalk depends on the amount of muscular contraction (subject movement), and the quality of the probes. It is well established that the amplitude of the Electromyographic signal is stochastic (random) in nature and can be reasonably modelled by a Gaussian distribution function. The mean of the noise can be assumed to be zero; however, the variance is dependent on the environmental variables and will change depending on the conditions. Certain studies have shown that the standard deviation of the noise is typically 10% of the peak-to-peak ECG amplitude. While the actual statistical model is unknown, it should be noted that the electrical activity of muscles during periods of contraction can generate surface potentials comparable to those from the heart and could completely drown out the desired signal. The frequency of this EMG noise is in between 100-500 Hz.

2.4.5 Instrumentation Noise

The electrical equipments used in ECG measurements also contribute noise. The major sources of this form of noise are the electrode probes, cables, signal processor or amplifier, and the analog-to-digital converter. Unfortunately instrumentation noise cannot be eliminated as it is inherent in electronic components, but it can be reduced through higher quality equipment and careful circuit design. Another form of noise, called flicker noise, is very important in ECG measurements, due to the low frequency content of ECG data. The actual mechanism that causes this type of noise is not yet understood, but one widely accepted theory is that it is caused by the energy traps which occur between the interfaces of two materials. It is believed that the charge carriers get randomly trapped/released and cause flicker noise.

2.5 ECG DATABASE

Since 1975, the laboratories at Boston's Beth Israel Hospital (now the Beth Israel Deaconess Medical Centre) and at Massachusetts Institute of Technology (MIT) have supported the research in arrhythmia analysis and related subjects by creating a database. One of the first major products of their effort was the Massachusetts Institute of Technology Beth Israel Hospital (MIT-BIH) database. This database was completed and began distributing in 1980. The database was the first generally available set of standard test material for evaluation of arrhythmia detectors and has been used for that purpose as well as for basic research into cardiac dynamics at more than 500 sites worldwide [26].

The MIT-BIH Arrhythmia Database contains 48 half-hour excerpts of two-channel ambulatory ECG recordings. These are obtained from 47 subjects collected by from a mixed population of inpatients (about 60%) and outpatients (about 40%) studied by the BIH Arrhythmia Laboratory. The subjects were taken from, 25 men aged 32 to 89 years and 22 women aged 23 to 89 years. About half (25 of 48 complete records and reference annotation files for all 48 records) of this database has been freely available in PhysioNet's inception in September 1999 [27]. The 23 remaining signal files, which had been available only on the MIT-BIH Arrhythmia Database CD-ROM, were posted in February 2005 [28]. The recordings were digitized at 360 samples per second per channel with 11-bit resolution over a 10 mV range.

Chapter 3

ECG Denoising Algorithms

Window based FIR filtering

Adaptive filtering

Wavelet filter bank

All the algorithms which are implemented in this thesis for ECG enhancement purpose are described here. For denoising purpose, the window based FIR filtering, adaptive filtering and wavelet filter bank based denoising are used.

3.1 FIR FILTERING

Digital filters are classified either as Finite Impulse Response (FIR) filters or Infinite Impulse response (IIR) filters, depending on the form of unit pulse response of the system. In the FIR system, the impulse response is of finite duration where as in the IIR system, the impulse response is of infinite duration. IIR filters are usually implemented using structures having feedback, that's why the present response of IIR filter is a function of present and past values of the excitation as well as the past value of the response. But the response of the FIR filter usually implemented using structures having no feedback so the response depends only on the present and past values of the input only [29]. The design of FIR filters is preferred due to the following advantages:

- Exact linear phase
- Always stable
- Design methods are linear
- Can be realized efficiently in hardware
- Filter start-up transients have finite duration

3.1.1 Design Techniques of FIR Filters

The FIR filter is implemented in a non-recursive way which guarantees a stable filter. FIR filter design mainly consists of two parts

i. Approximation part
ii. Realization part

In the approximation stage, the specifications of the filters are taken and a transfer function is generated. In approximation, first an ideal frequency response is taken of length N (N represents the order of the FIR filter). Then a method or algorithm is selected for the implementation of the filter transfer function.

In the realization part, a structure is chosen to implement the transfer function i.e. in the form of circuit diagram or a program.

There are essentially three well-known methods for FIR filter design namely:

i. The window method
ii. The frequency sampling technique
iii. Fourier series method

In our work, we have used the window method of FIR filter design for noise reduction. The window method of filter design is discussed in the following section.

3.1.2 The Window Based FIR Filter Design

In this method, we start with the desired frequency response specification $H_d(\omega)$ and the corresponding unit sample response $h_d(n)$ is determined using inverse Fourier transform. The relation between $H_d(\omega)$ and $h_d(n)$ is as follows :

$$H_d(\omega) = \sum_{i=0}^{\infty} h_d(n) e^{-j\omega n} \tag{3.1}$$

Where

$$h_d(n) = \int_{-\pi}^{\pi} H_d(\omega) e^{j\omega n} \, d\omega \tag{3.2}$$

The impulse response $h_d(n)$ obtained from the Eq. 3.2 is of infinite duration. So, it is truncated at some point, say n = M - 1 to yield an FIR filter of length M (i.e. 0 to M-1). This truncation of $h_d(n)$ to length M - 1 is done by multiplying $h_d(n)$ with an window . Here the design is explained by considering the “rectangular window”, defined as

$$w(n) = \begin{cases} 1 & n = 0,1,2......M-1 \\ 0 & \text{otherwise} \end{cases} \tag{3.3}$$

Thus, the impulse response of the FIR filter becomes

$$\begin{aligned} h(n) &= h_d(n)\, w(n) \\ &= \begin{cases} h_d(n) & n = 0,1,2......M-1 \\ 0 & \text{otherwise} \end{cases} \end{aligned} \tag{3.4}$$

Now, the multiplication of the window function $w(n)$ with $h_d(n)$ is equivalent to convolution of $H_d(\omega)$ with $W(\omega)$, where $W(\omega)$ is the frequency domain representation (Fourier transform) of the window function i.e.

$$W(\omega) = \sum_{i=0}^{\infty} w(n)\, e^{-j\omega n} \tag{3.5}$$

Thus, the convolution of $H_d(\omega)$ with $W(\omega)$ yields the frequency response of the truncated FIR Filter $H(\omega)$.

$$H(\omega) = \frac{1}{2\pi} \int_{-\pi}^{\pi} H_d(v) W(\omega - v)\, dv \tag{3.6}$$

The frequency response can also be obtained by Fourier transform of $h(n)$, given in the following relation

$$H(\omega) = \sum_{i=0}^{\infty} h(n)\, e^{-j\omega n} \tag{3.7}$$

But direct truncation of the Fourier series $h_d(n)$ to M terms to obtain $h(n)$ is known to introduce ripples in the frequency response characteristic $H(\omega)$. It is due to the nonuniform convergence of the Fourier series at a discontinuity. The Oscillatory behaviour near the band edge of the filter is called *Gibbs phenomenon*. Thus, the frequency response obtained using Eq. 3.7 contains ripples in the frequency domain [30].

In order to reduce the ripples, $h_d(n)$ is multiplied with a window function that contains a taper and decays toward zero gradually instead of abruptly as it occurs in a rectangular window. As multiplication of sequences $h_d(n)$ and $w(n)$ in time domain is equivalent to convolution of $H_d(\omega)$and $W(\omega)$ in the frequency domain, it has the effect of smoothing $H_d(\omega)$.

The several effects of windowing the Fourier coefficients on the frequency response of the filter are as follows [31]:

- A major effect is the discontinuities in $H_d(\omega)$.
- The width of the transition bands depends on the width of the main lobe of the frequency response of the window function $w(n)$ i.e. $W(\omega)$.
- Since, the filter frequency response is obtained via a convolution relation, it is clear that the resulting filters are never optimal in any sense.

- As M (the length of the window function) increases, the main lobe width of $W(\omega)$ is reduced which reduces the width of the transition band, but this also introduces more ripple in the frequency response.
- The window function eliminates the ringing effects at the band edge and does result in lower side lobes at the expense of an increase in the width of the transition band of the filter.

The major advantages of using window method are their relative simplicity and ease of use as compared to other methods. The fact that well defined equations are often available for calculating the window coefficients has made this method successful.

There are following problems in filter design using window method [32]:

- This method is applicable only if $H_d(\omega)$ is absolutely integrable, i.e. only if Eq. 3.2 can be evaluated. When $H_d(\omega)$ is complicated or cannot easily be put into a closed form mathematical expression, evaluation of $h_d(n)$ becomes difficult.
- The use of windows offers very little design flexibility, e.g. in low-pass filter design, generally the pass band edge frequency cannot be specified exactly, since the window smears the discontinuity in frequency. Thus, the ideal LPF with cut-off frequency f_c, is smeared by the window to give a frequency response with pass band response with pass band cut off frequency f_1 and stop band cut-off frequency f_2.
- Window method is basically useful for design of prototype filters like low pass, high pass, band pass, etc. This makes its applications very limited.

There are different types of windows present [30]. The windows used in our work for design of FIR filters are [33]

- *Rectangular window:*

$$W_R(n) = \begin{cases} 1 & 0 \le n \le M-1 \\ 0 & \text{otherwise} \end{cases} \tag{3.8}$$

- *Hanning window:*

$$W_{hn}(n) = \begin{cases} 0.5 - 0.5 * \cos\left(\dfrac{2\pi n}{M-1}\right) & 0 \le n \le M-1 \\ 0 & \text{otherwise} \end{cases} \tag{3.9}$$

- *Hamming window :*

$$W_{hm}(n)=\begin{cases}0.54-0.46*\cos\left(\dfrac{2\pi n}{M-1}\right) & 0\le n\le M-1\\ 0 & \text{otherwise}\end{cases} \tag{3.10}$$

- *Blackman window :*

$$W_B(n)=\begin{cases}0.42-0.5*\cos\left(\dfrac{2\pi n}{M-1}\right) & 0\le n\le M-1\\ 0 & \text{otherwise}\end{cases} \tag{3.11}$$

3.2 ADAPTIVE FILTERING

Adaptive filtering involves the change of filter parameters (coefficients) over time. It adapts to the change in signal characteristics in order to minimize the error. It finds its application in adaptive noise cancellation, system identification, frequency tracking and channel equalization [34]. Fig. 3.1 shows the general structure of an adaptive filter.

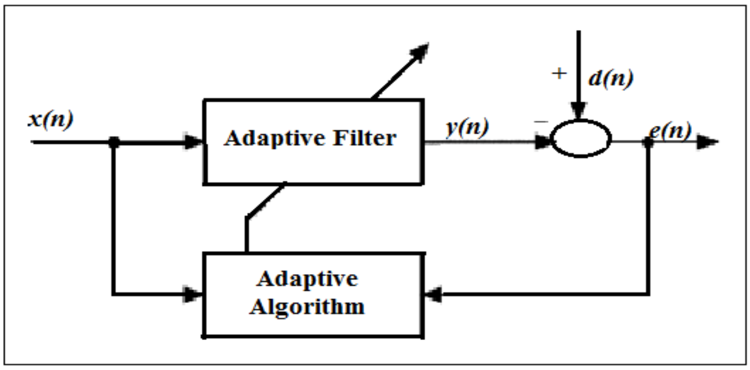

Figure 3.1 Adaptive filter structure

In Fig. 3.1, *x(n)* denotes the input signal. The vector representation of *x(n)* is given in Eq. 3.12. This input signal is corrupted with noises. In other words, it is the sum of desired signal *d(n)* and noise *v(n)*, as mentioned in Eq. 3.13.

The input signal vector is *x(n)* which is given by

$$x(n)=[x(n),x(n-1),.......x(n-N-1)]^T \tag{3.12}$$

$$x(n)=d(n)+v(n) \tag{3.13}$$

The adaptive filter has a Finite Impulse Response (FIR) structure. For such structures, the impulse response is equal to the filter coefficients. The coefficients for a filter of order N are defined as

$$W(n) = [w_n(0),\ w_n(1),\ ......w_n(N-1)]^T \tag{3.14}$$

The output of the adaptive filter is *y(n)* which is given by

$$y(n) = W(n)^T x(n) \tag{3.15}$$

The error signal or cost function is the difference between the desired and the estimated signal

$$e(n) = d(n) - y(n) \tag{3.16}$$

Moreover, the variable filter updates the filter coefficients at every time instant

$$W(n+1) = W(n) + \Delta W(n) \tag{3.17}$$

where $\Delta W(n)$ is a correction factor for the filter coefficients. The adaptive algorithm generates this correction factor based on the input and error signals [35].

3.2.1 Adaptive Algorithms

In adaptive filters, the weight vectors are updated by an adaptive algorithm to minimize the cost function. The algorithms used by us for noise reduction in ECG in this thesis are least mean square (LMS), Normalized least mean square (NLMS), sign data least mean square (SDLMS), sign error least mean square (SELMS) and sign-sign least mean square (SSLMS) algorithms [34].

3.2.1.1 LMS algorithm

It is a stochastic gradient descent method in which the filter weights are only adapted based on the error at the current time. According to this LMS algorithm the updated weight is given by

$$W(n+1) = W(n) + 2.\mu.x(n).e(n) \tag{3.18}$$

where μ is the step size.

3.2.1.2 NLMS algorithm

The NLMS algorithm is a modified form of the standard LMS algorithm. The NLMS algorithm updates the coefficients of an adaptive filter by using the following equation

$$W(n+1) = W(n) + 2.\mu.\frac{x(n)}{\|x(n)\|^2}.e(n) \tag{3.19}$$

Eq. 3.19 can be rewritten as

$$W(n+1) = W(n) + 2.\mu(n).x(n).e(n) \tag{3.20}$$

where $\mu(n) = \frac{\mu}{\|x(n)\|^2}$

From Eq. 3.18 and Eq. 3.20, the NLMS algorithm becomes the same as the standard LMS algorithm except that the NLMS algorithm has a time-varying step size $\mu(n)$. This step size improves the convergence speed of the adaptive filter.

3.2.1.3 SDLMS algorithm

In SDLMS algorithm, the sign function is applied to the input signal vector *x(n)*. This algorithm updates the coefficients of an adaptive filter using the following equation

$$W(n+1) = W(n) + 2.\mu.\mathrm{sgn}(x(n)).e(n) \tag{3.21}$$

3.2.1.4 SELMS algorithm

In SELMS, the sign function is applied to the error signal *e(n)*. This algorithm updates the coefficients of an adaptive filter using the following equation

$$W(n+1) = W(n) + 2.\mu.x(n).\mathrm{sgn}(e(n)) \tag{3.22}$$

3.2.1.5 SSLMS algorithm

Here, the sign function is applied to both $e(n)$ and *x(n)*. This algorithm updates the coefficients of an adaptive filter using the following equation

$$W(n+1) = W(n) + 2.\mu.\mathrm{sgn}(x(n)).\mathrm{sgn}(e(n)) \tag{3.23}$$

3.3 WAVELET DENOISING

The wavelet transform is similar to the Fourier transform. For the FFT, the basis functions are sines and cosines. For the wavelet transform, the basis functions are more complicated called wavelets, mother wavelets or analyzing wavelets and scaling function. In wavelet analysis, the signal is broken into shifted and scaled versions of the original (or *mother*) wavelet. The fact that wavelet transform is a multiresolution analysis makes it very suitable for analysis of non-stationary signals such as the ECG signal [40].

3.3.1 Wavelet Transform

The Fourier transform is useful tool to analyze the frequency components of the signal. However, if we take the Fourier transform over the whole time axis, we cannot tell at what instant a particular frequency rises. Short-time Fourier transform (STFT) uses a sliding window to find spectrogram, which gives the information of both time and frequency. But still another problem exists i.e. the length of window limits the resolution in frequency. Wavelet transform seems to be a solution to the problem above. Wavelet transforms (WT) are based on small wavelets with limited duration. In WT both the time and frequency resolutions vary in time-frequency plane in order to obtain a multiresolution analysis.

In wavelet transform, a signal $x(t)$ which belongs to the square integrable subspace $L^2(R)$ is expressed in terms of scaling function $\varphi_{j,k}(t)$ and mother wavelet function $\psi_{j,k}(t)$. Here j is the parameter of dilation or the visibility in frequency and k is the parameter of the position.

$$x(t)=\sum_{k} a_{j_0,k}\, \varphi_{j_0,k}(t)+\sum_{j=j_0}^{\infty}\sum_{k} b_{j,k}\, \psi_{j,k}(t) \tag{3.24}$$

where a, b are the coefficients associated with $\varphi_{j,k}(t)$ and $\psi_{j,k}(t)$ respectively.

The coefficients a, b can be calculated as we calculate the coefficients in Fourier transform. The expression of a, b are given in the following equations

$$a_{j_0,k} = \int_{-\infty}^{\infty} x(t)\, \varphi_{j_0,k}(t)\, dt \tag{3.25}$$

$$b_{j,k} = \int_{-\infty}^{\infty} x(t)\psi_{j,k}(t)\,dt \tag{3.26}$$

The scaling function $\varphi_{j,k}(t)$ can be expressed as

$$\varphi_{j,k}(t) = 2^{j/2}\varphi\left(2^j t - k\right) \tag{3.27}$$

$\psi_{j,k}(t)$ can also be derived from its shifted version i.e. $\varphi_{j,k}(2t)$. The expression of $\varphi_{j,k}(t)$ in terms of $\varphi_{j,k}(2t)$ will be

$$\varphi(t) = \sum_n h_\varphi(n)\sqrt{2}\,\varphi(2t-n) \tag{3.28}$$

In Eq. 3.28, n is the shifting parameter and $h_\varphi(n)$ are the coefficients.

The mother wavelet function $\psi_{j,k}(t)$ is expressed as

$$\psi_{j,k}(t) = 2^{j/2}\psi\left(2^j t - k\right) \tag{3.29}$$

$\psi_{j,k}(t)$ can also be written using shifted version $\varphi_{j,k}(t)$ i.e. $\varphi_{j,k}(2t)$. The expression of $\psi_{j,k}(t)$ will be

$$\psi(t) = \sum_n h_\psi(n)\sqrt{2}\,\varphi(2t-n) \tag{3.30}$$

In Eq. 3.30, n is the shifting parameter and $h_\psi(n)$ are the coefficients.

3.3.2 Discrete Wavelet Transform

The discrete wavelet transform (DWT) is an implementation of the wavelet transform using a discrete set of the wavelet scales and translations obeying some defined rules. In other words, this transform decomposes the signal into mutually orthogonal set of wavelets.

The scaling function $\varphi_{j,k}(n)$ and the mother wavelet function $\psi_{j,k}(n)$ in discrete domain are

$$\varphi_{j,k}(n) = 2^{j/2}\varphi\left(2^j n - k\right) \tag{3.31}$$

$$\psi_{j,k}(n) = 2^{j/2}\psi\left(2^j n - k\right) \tag{3.32}$$

The DWT of an discrete signal *x(n)* of length *M-1* is given in the Eq. 3.33. It is quite similar to the Eq. 3.24.

$$x(n)=\sum_k W_\varphi(j_0,k)\,\varphi_{j_0,k}(n)+\sum_{j=j_0}^{\infty}\sum_k W_\psi(j_0,k)\,\psi_{j,k}(n) \tag{3.33}$$

here $W_\varphi(j_0,k)$ and $W_\psi(j_0,k)$ are called the wavelet coefficients.

$\varphi_{j,k}(n)$ and $\psi_{j,k}(n)$ are orthogonal to each other. Hence we can simply take the inner product to obtain the wavelet coefficients.

$$W_\varphi[j_0,k]=\frac{1}{\sqrt{M}}\sum_n x(n)\,\varphi_{j_0,k}[n] \tag{3.34}$$

$$W_\psi[j,k]=\frac{1}{\sqrt{M}}\sum_n x(n)\,\psi_{j_0,k}[n] \quad j\geq j_0 \tag{3.35}$$

The above two equations are quite similar to Eq. 3.25 and Eq. 3.26 except $1/\sqrt{M}$, which can be taken as normalization term.

The coefficients $W_\varphi(j_0,k)$ are called the approximation coefficients and the coefficients $W_\psi(j_0,k)$ are called the detailed coefficients. The DWT can be realized in terms of high pass and low pass filters. The approximation properties of filter banks and their relation to wavelets are presented in the paper [44]. The output of the low pass filter gives the approximation coefficients and the output of the high pass filter gives the detailed coefficients. To get the filter coefficients $W_\varphi(j_0,k)$ and $W_\psi(j_0,k)$ can be rewritten as

$$W_\varphi(j,k)=\sum_n h_\varphi(n-2k)W_\varphi(j+1,m) \tag{3.36}$$

$$W_\psi(j,k)=\sum_m h_\psi(m-2k)W_\psi(j+1,m) \tag{3.37}$$

h_φ and h_ψ are the filter coefficients of the low pass filter and high pass filter respectively.

Computation of the wavelet coefficients at every possible scale is a fair amount of work and it generates an awful lot of data. Selection of a subset of scales and positions based on powers of two (dyadic scales and positions) results in a more efficient and accurate analysis. Mallat [42], [43] has introduced repetitive application of *high pass* and *low pass* filters to calculate the wavelet expansion of a given sequence of discrete numbers.

3.3.3 Wavelet Decomposition

The DWT decomposes the signal into approximate and detail information as discussed in section 3.3.2. Thus, it helps in analyzing the signal at different frequency bands with different resolutions.

3.3.3.1 Single stage wavelet filtering

In single stage wavelet filtering the original signal *x(n)* is passed through two complementary filters and emerges as two signals. The filtering process, at its most basic level is shown in Fig. 3.2.

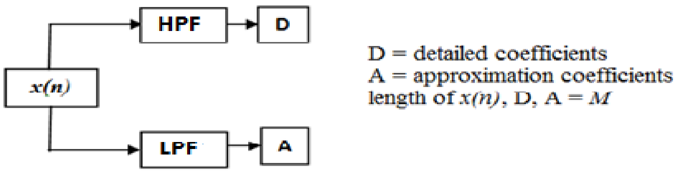

Figure 3.2 Single stage wavelet filtering

If single stage wavelet filter is applied on a digital signal, then we end with twice as much data as we started with. The original signal *x(n)* consists of *M* samples of data. The resulting approximation and detail coefficients are each of length *M*, for a total of *2M*.

There exists an alternative method to perform the decomposition using wavelets. By down sampling A and D to half of their lengths i.e. *M/2*, the total length of resulting signal can be maintained. The final output signals after down sampling are denoted as cA and cD. It is diagrammatically shown in Fig. 3.3.

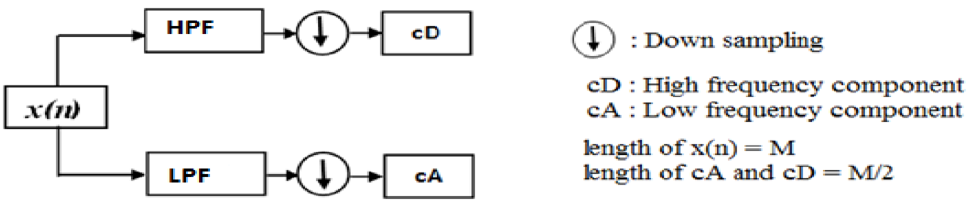

Figure 3.3 Single stage wavelet filtering with down sampling

3.3.3.2 Multistage wavelet filtering

The wavelet decomposition process can be iterated, so that one signal is broken down into many lower resolution components. This is called the *wavelet decomposition tree*.

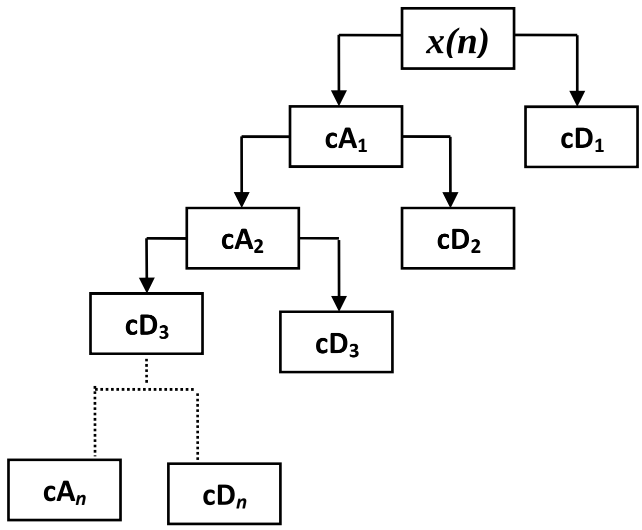

Figure 3.4 multistage wavelet decomposition tree

Since multistage wavelet filtering analysis process is iterative, theoretically it can be continued till infinite levels. Ideally the decomposition can be done only until the individual details consist of a single sample. In practice, a suitable number of decomposition levels based on the nature and frequency component of the signal.

3.3.4 Wavelet Reconstruction

In section 3.3.3, the analysis of a signal by discrete wavelet transform decomposition is discussed. This process is called *decomposition* or *analysis*. After decomposition, the task is to again reconstruct the original signal without loss of important information. This process is called *reconstruction*, or *synthesis*. The synthesis is done mathematically by using the inverse discrete wavelet transform (IDWT).

In wavelet analysis, filtering and followed by down sampling are involved. But the wavelet reconstruction process consists of up sampling followed by filtering. Up sampling is the process of lengthening a signal component by inserting zeros between samples.

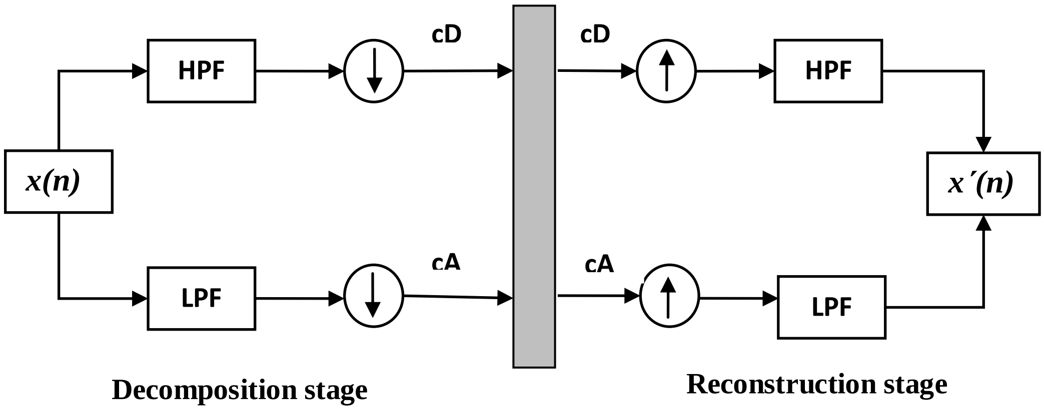

Figure 3.5 single stage decomposition and reconstruction

We combine cA and cD by IDWT to get the reconstructed original signal. However, instead of combining, we can feed a vector of zeros in place of the detail coefficients vector or approximation coefficients as per our requirement. For example, when cD is made zero before combining with cA, it yields a reconstructed *approximation* A1. A1 has the same length as the original signal *x(n)* and which is a real approximation of it.

For multiple level reconstruction, the single stage reconstruction technique is iterated to reassemble the original sinal.

3.3.5 ECG Denoising Using Wavelet Transform

In this proposed method, the corrupted ECG signal *x(n)* is denoised by taking the DWT of raw and noisy ECG signal. A family of the mother wavelet is available having the energy spectrum concentrated around the low frequencies like the ECG signal as well as better resembling the QRS complex of the ECG signal. We have used *symlet* wavelet, which resembles the ECG wave.

In discrete wavelet transform (DWT), the low and high frequency components in *x(n)* is analyzed by passing it through a series of low-pass and high-pass filters with different cut-off frequencies. This process results in a set of approximate coefficients (cA) and detail coefficients (cD). To remove the power line interference and the high frequency noise, the DWT is computed to level 4 using *symlet8* mother wavelet function and scaling function. Then the approximate coefficients at level 4 (cA_4) are set to zero. After that, inverse wavelet transform (IDWT) of the modified coefficients are taken to obtain the approximate noise of the ECG signal. The residue of the raw signal and the approximate noise is obtained to get noise free ECG signal.

Chapter 4

Results and Discussion

Window based FIR filtering

Adaptive filtering

Wavelet filter bank based denoising

In this chapter, all the simulation results using the algorithms discussed in chapter 3 are presented under different subsections. The ECG waveform taken from MIT-BIH database, generated noises and the corrupted ECG signal are also shown.

4.1 ECG WAVEFORM

All the simulations shown in the later parts are carried out with data no. 100 of MIT-BIH arrhythmia database. The ECG waveform is shown in Fig. 4.1.

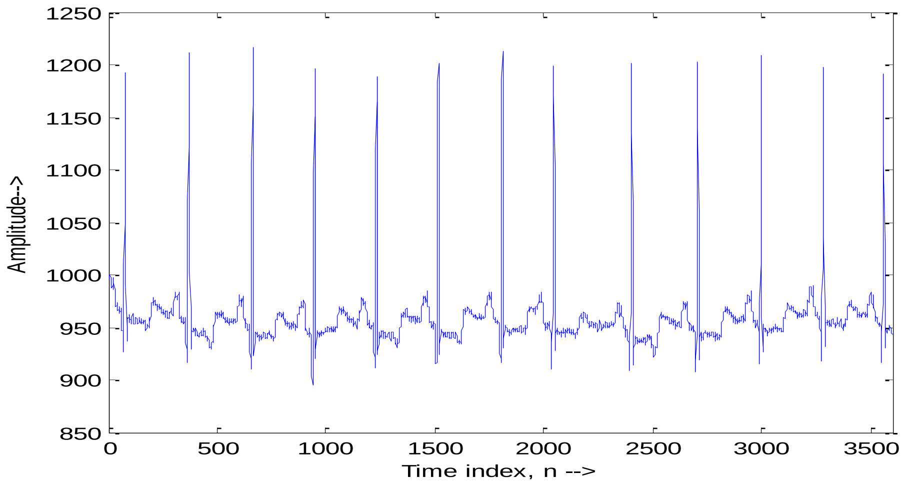

Figure 4.1 ECG Signal from MITBIH arrhythmia database

4.2 GENERATION OF NOISES

The artifacts in ECG can be categorized according to their frequency content. The low frequency noise (electrode contact noise and motion artifact) has frequency less than 1 Hz, high frequency noise (EMG noise) whose frequency is more than 100 Hz and power line interference of frequency 50 Hz or 60 Hz (depending on the supply). These noises are generated in MATLAB based on their frequency content.

4.2.1 Generation of Low Frequency Noise (Base Line Wander)

We generated the baseline drift by adding two sine waves of frequency 0.1 Hz and 0.02 Hz and triangular wave of 0.05 Hz which is shown in Fig. 4.2.

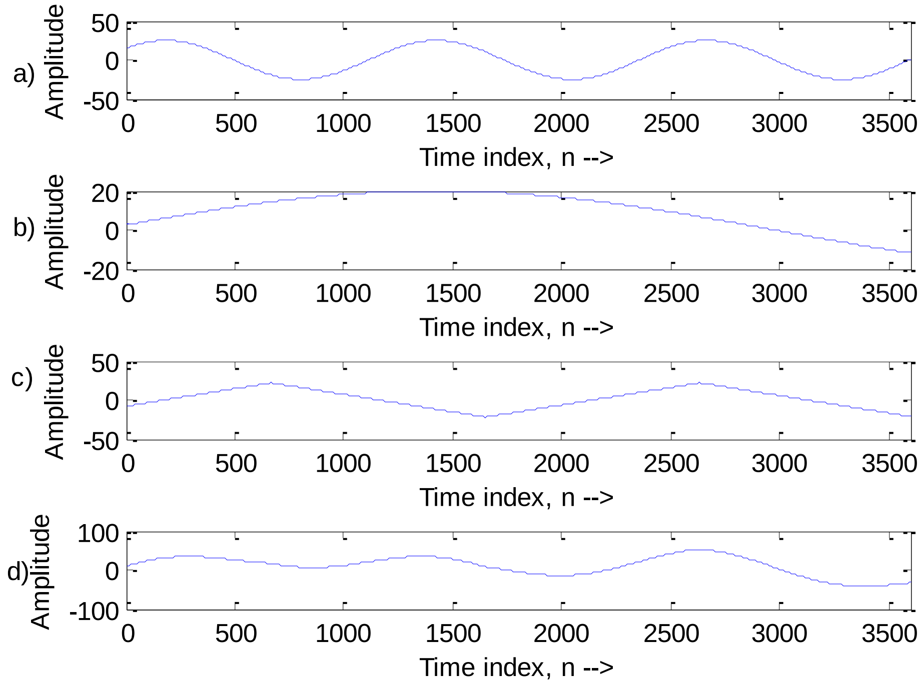

Figure 4.2 a) sine wave of frequency 0.1 Hz b) sine wave of frequency 0.02 Hz c)triangular wave of frequency 0.05Hz d) base line wander

4.2.2 Generation of High Frequency Noise

High frequency noise is generated by multiplying sine wave of 150 Hz frequency with a random signal. The generated high frequency noise is shown in Fig. 4.3.

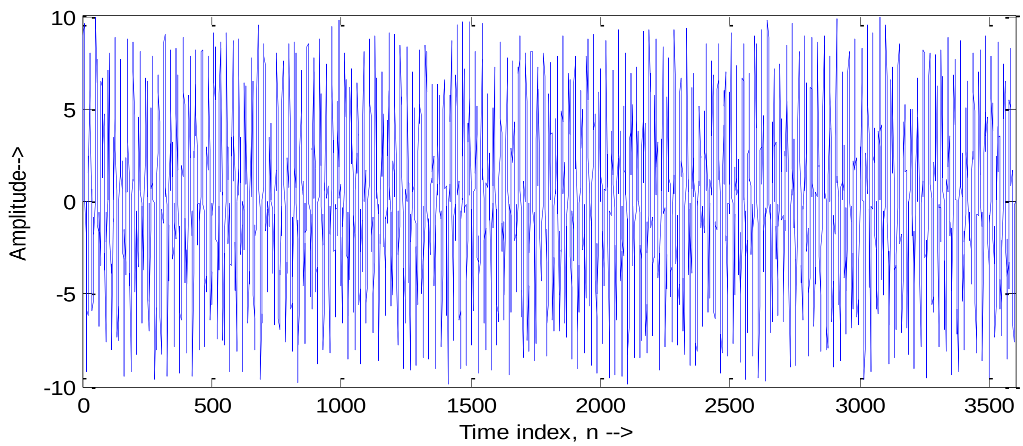

Figure 4.3 High frequency noise

4.2.3 Generation of Power Line Interference

Here the 50 Hz power supply is considered. So, a sine wave of 50 Hz amplitude was taken to represent the power line interference. The resulted power line interference is shown in Fig. 4.4.

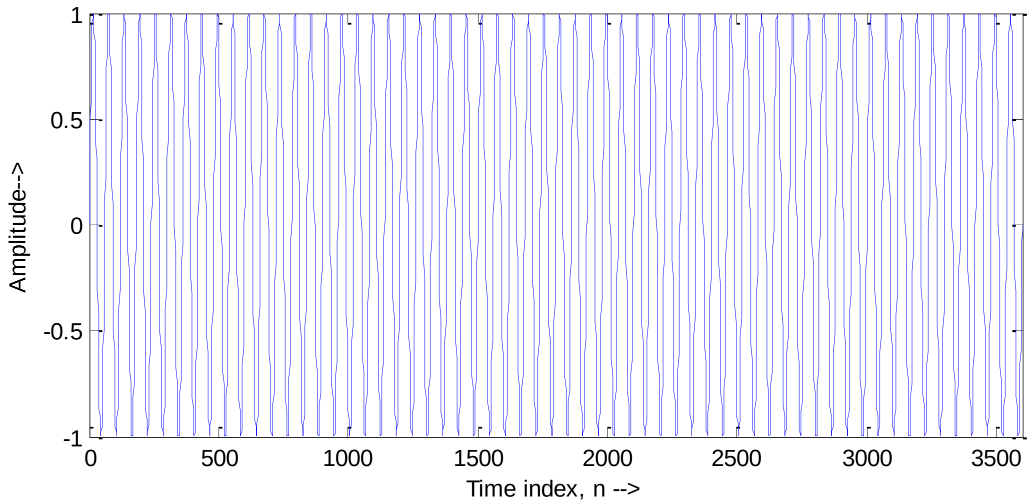

Figure 4.4 Power line interference

4.3 ADDITION OF NOISES TO ECG

The noise signals generated are added with the ECG signal to get the corrupted ECG. Fig. 4.5 shows the corrupted ECG.

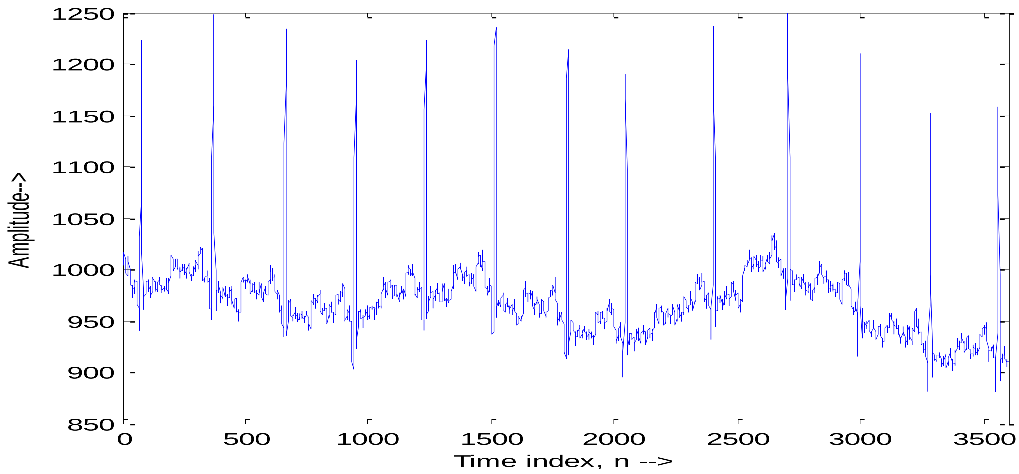

Figure 4.5 Corrupted ECG signal

4.4 RESULTS OF WINDOW BASED FIR FILTERING

We designed the filters of order 100. In rectangular window based FIR filter response, it was clear that the filter has sharp attenuation and pulsation in the stop band. In the pass band, the filter was found to be stable. The Hamming, Hanning and the Blackman windows do not have a sharp cut-off like the Rectangular window. Using these windows, we designed the high pass filter of cut-off frequency 3 Hz and the low pass filter of cut-off frequency 100Hz. Fig. 4.6, 4.7, 4.8, 4.9 show the filtered ECG signal by passing through the FIR filter based on Rectangular window, Hamming window, Hanning window and Blackman window respectively.

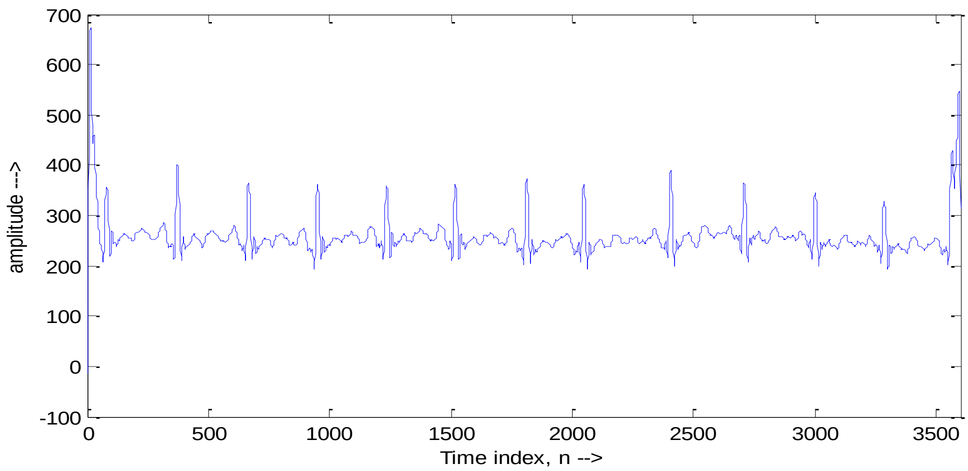

Figure 4.6 ECG signal after passing through FIR filter with Rectangular Window

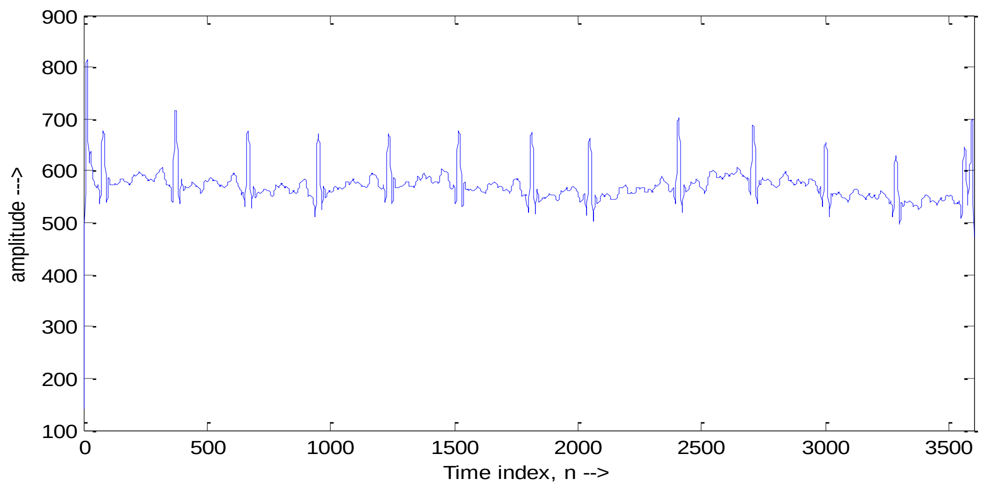

Figure 4.7 ECG signal after passing through FIR filter with Hamming window

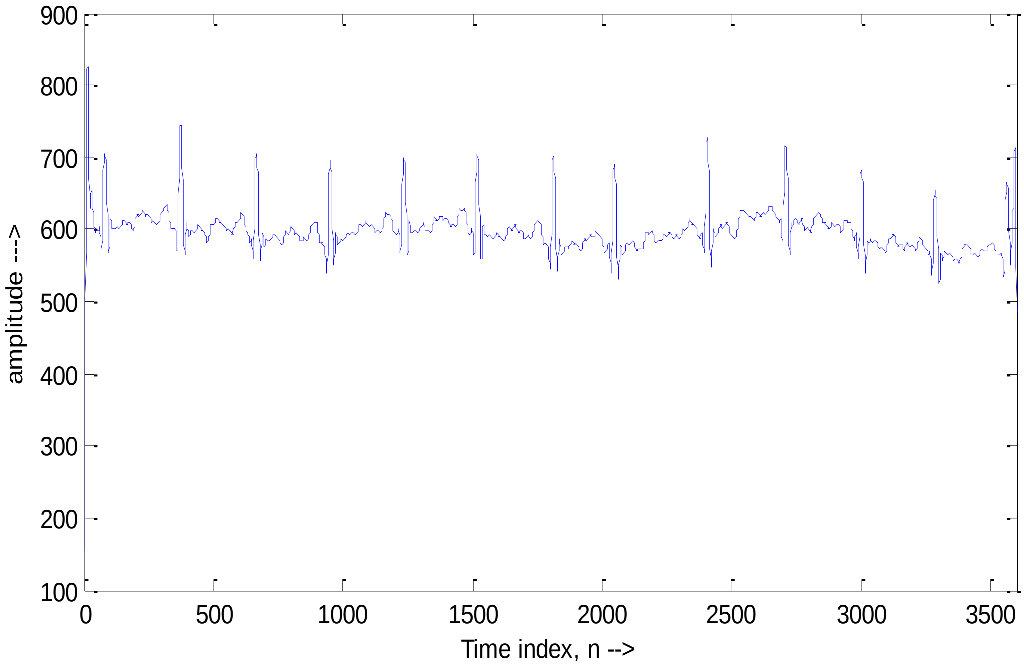

Figure 4.8 ECG signal after passing through FIR filter with Hanning window

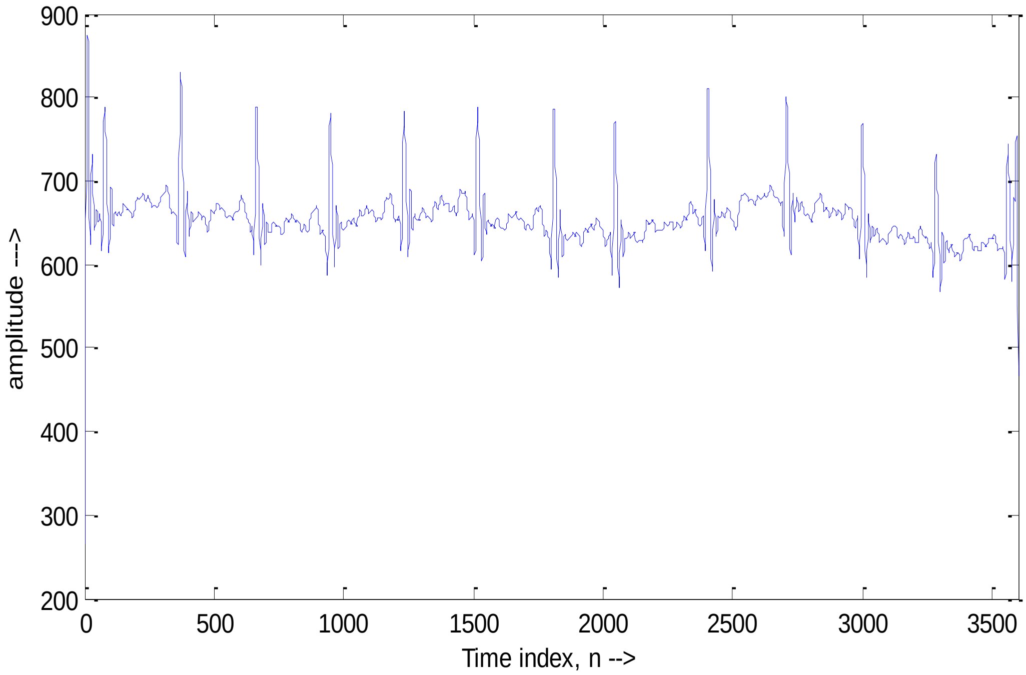

Figure 4.9 ECG signal after passing through FIR filter with Blackman window

To quantify the performance of all these filters the PSNRs were calculated which is listed in the table 4.1.

Table 4.1 PSNR comparison of window based FIR filters

Widow Type	PSNR(dB)
Rectangular	20.31
Hanning	17.65
Hamming	17.90
Blackman	18.01

The performance of rectangular window based filter is better than the rest window based filters as the rectangular filter has sharp attenuation and pulsation present in the stop band. The phase response of rectangular window based filter is linear and the filter is also stable.

4.5 RESULTS OF ADAPTIVE FILTERING

The corrupted signal shown in Fig. 4.5 is passed through the adaptive filters. Fig. 4.10, 4.11, 4.12, 4.13 and 4.14 show the filtered output and the error plot of the adaptive filters using LMS, NLMS, SDLMS, SELMS, SSLMS algorithms respectively.

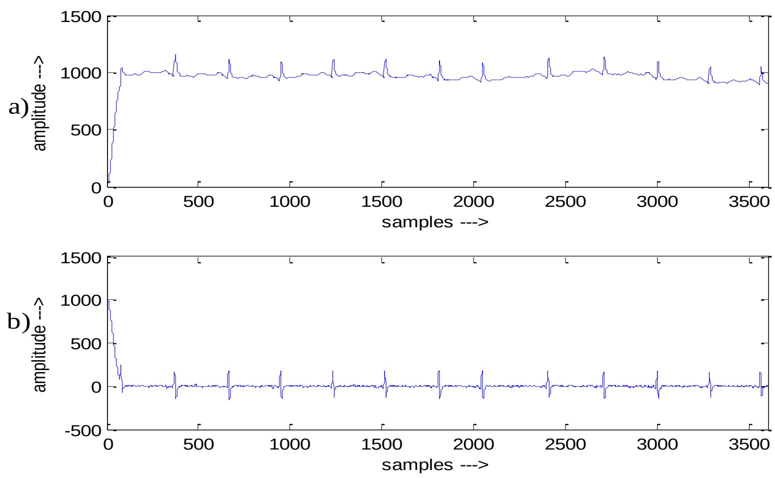

Figure 4.10 (a) ECG signal after passing through LMS based filter (b) Error plot after passing through LMS based adaptive filter

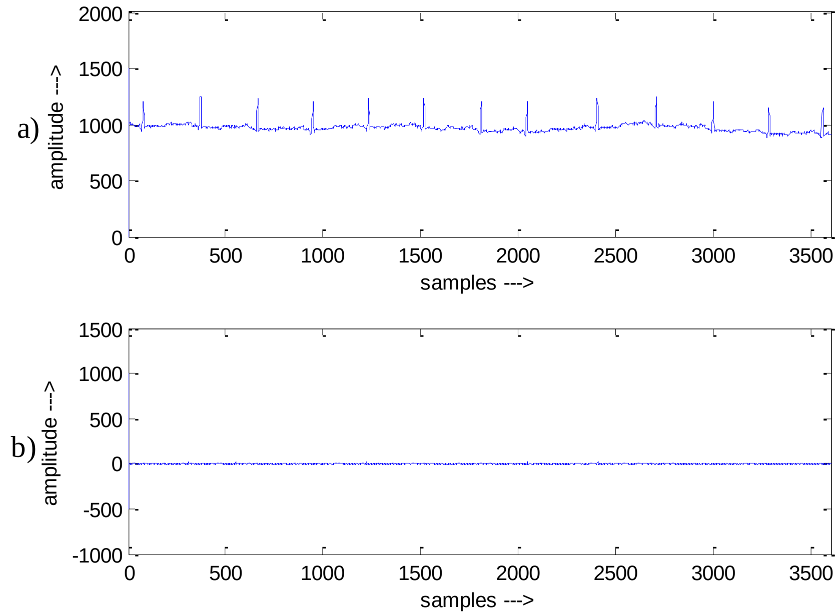

Figure 4.11 (a) ECG signal after passing through NLMS based filter (b) Error plot after passing through NLMS based adaptive filter

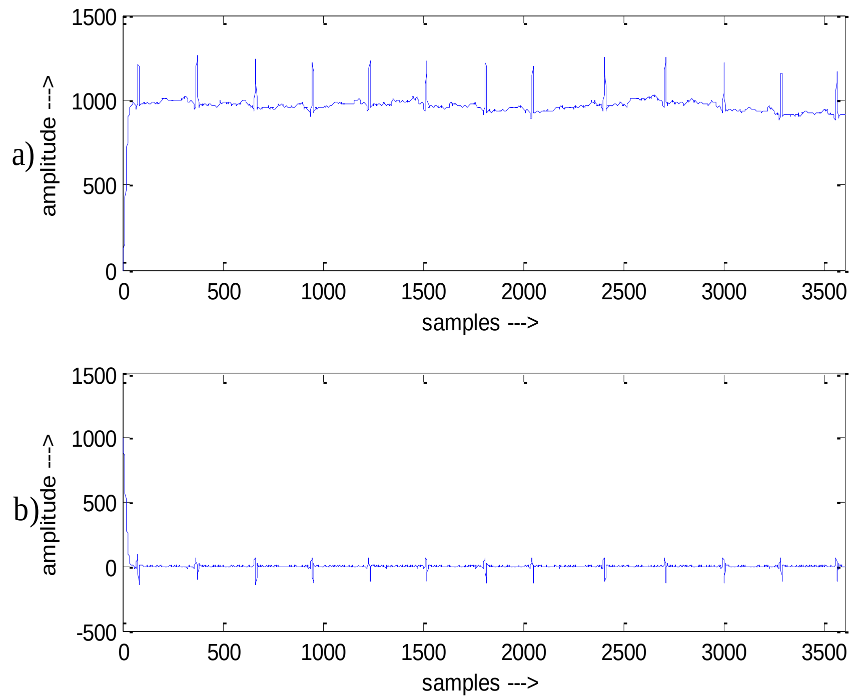

Figure 4.12 (a) ECG signal after passing through SDLMS based filter (b) Error plot after passing through SDLMS based adaptive filter

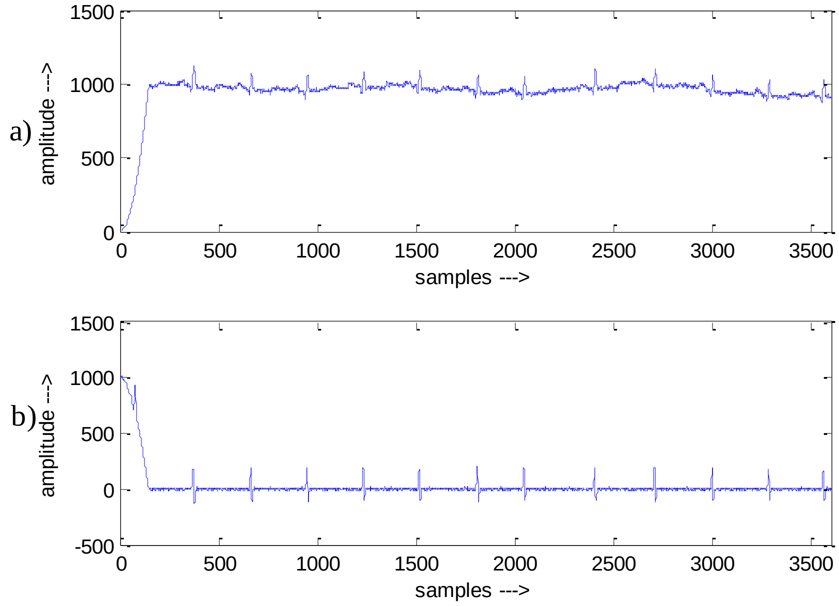

Figure 4.13 (a) ECG signal after passing through SELMS based filter (b) Error plot after passing through SELMS based adaptive filter

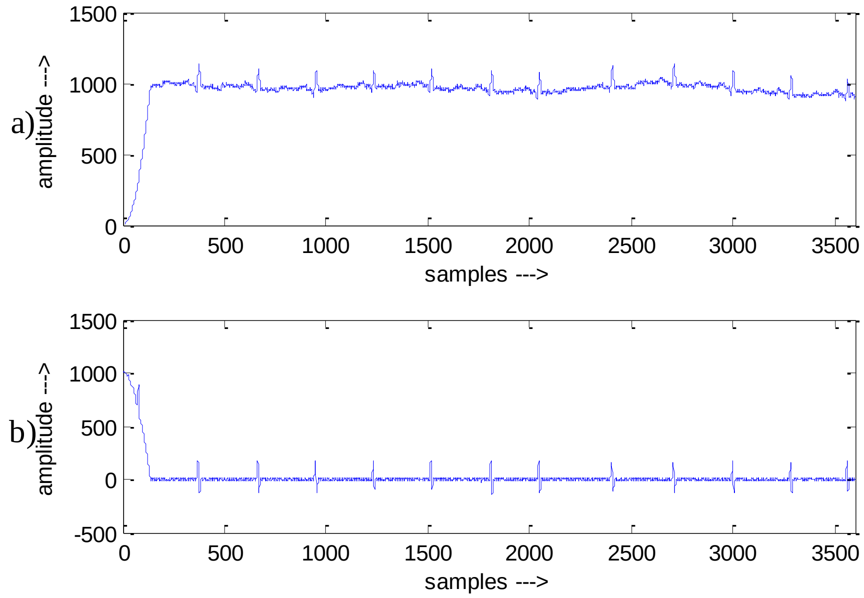

Figure 4.14 (a) ECG signal after passing through SSLMS based filter (b) Error plot after passing through SSLMS based adaptive filter

All the simulations shown in the above figures are carried out with data no. 100 of MIT-BIH arrhythmia database. To have a comparison of these adaptive filters, the PSNR values are calculated with ECG data 105 and 108 of the database. PSNR values of different adaptive filters are shown in Table 4.2.

Table 4.2 : PSNR values of various adaptive filters

Data No.	LMS	NLMS	SDLMS	SELMS	SSLMS
100	35.5707	38.2398	37.2995	34.6284	31.3315
105	35.1094	37.4581	35.2212	34.1698	32.5258
108	32.4158	35.3557	31.8226	31.8515	32.5244
average	34.3653	37.0178	34.7811	33.5499	32.1272

From the comparative analysis of the PSNR values, it can be inferred that the NLMS based adaptive filter gives the best result amongst all. In case of SDLMS, SELMS and SSLMS based adaptive filters, the computational complexity is decreased at the cost of lower PSNR values. So, NLMS algorithm is preferred when better performance is required. Sign based adaptive algorithms are chosen when faster performance is needed.

4.6 RESULTS OF WAVELET FILTER BANK BASED DENOISING

For wavelet filter bank based denoising, we have only considered the high frequency noise and the power line interference shown in Fig. 4.3 and Fig. 4.4. These noises are added to the ECG signal shown in Fig. 4.1. After adding the noises, the corrupted ECG signal is shown in Fig. 4.15.

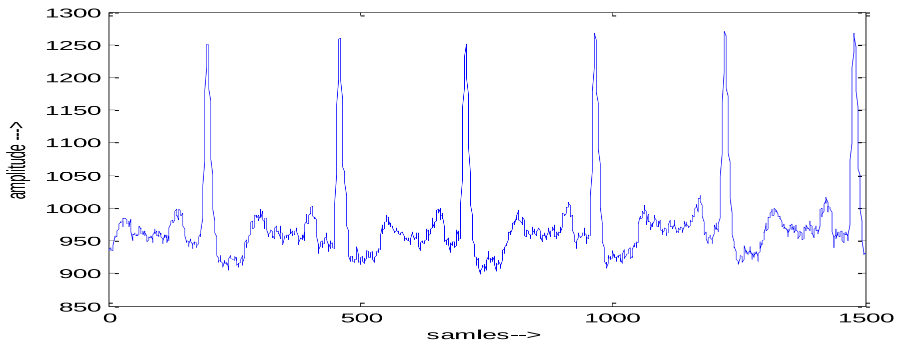

Figure 4.15 Noisy ECG signal used in wavelet filter bank based denoising

The noisy signal shown in Fig. 4.14 is denoised by using discrete wavelet transform. For this, we have chosen *symlet8* wavelet because it has energy spectrum concentrated around the low frequencies like the ECG signal. The *symlet8* wavelet also resembles the QRS complex of the ECG signal. The scaling function φ and wavelet function ψ are shown in Fig. 4.16 and Fig. 4.17.

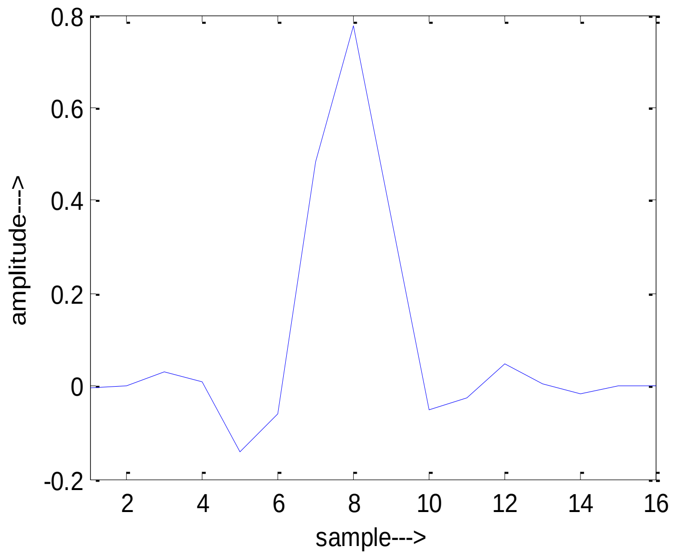

Figure 4.16 Symlet scaling function φ

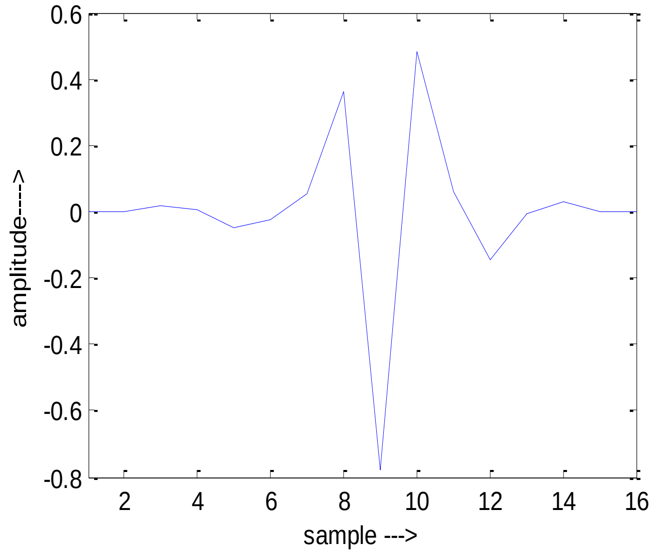

Figure 4.17 Symlet wavelet function ψ

To remove the power line interference and the high frequency noise, the DWT is computed to level 4 using *symlet8* mother wavelet function and scaling function. The approximate coefficients cA_n and cD_n at each decomposition level are shown in Fig. 4.18 and Fig. 4.19 respectively.

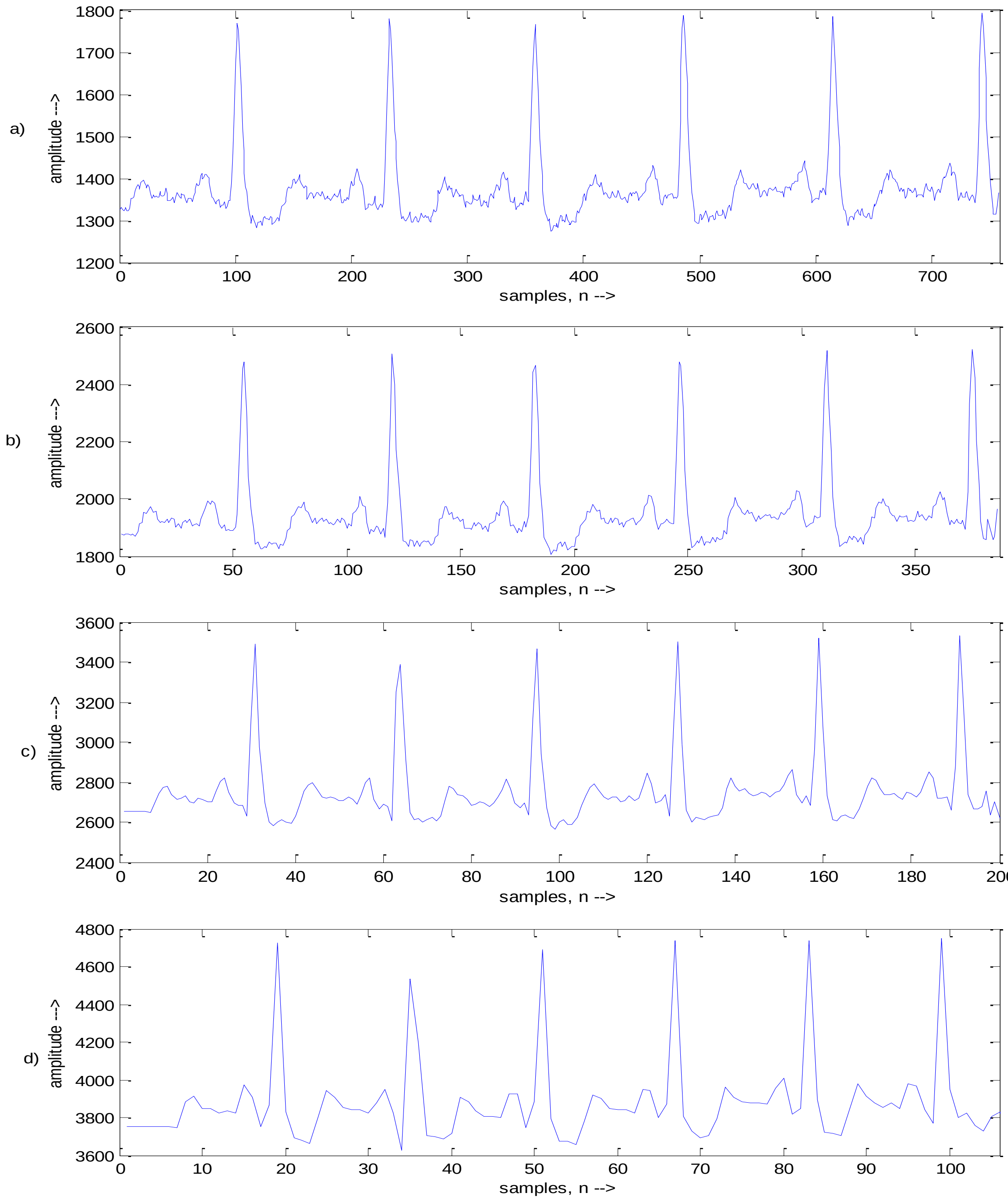

Figure 4.18 Approximation coefficients a) cA_1 : approximation coefficients at level 1, b) cA_2 : approximation coefficients at level 2, c) cA_3 : approximation coefficients at level 3, d) cA_4 : approximation coefficients at level 4

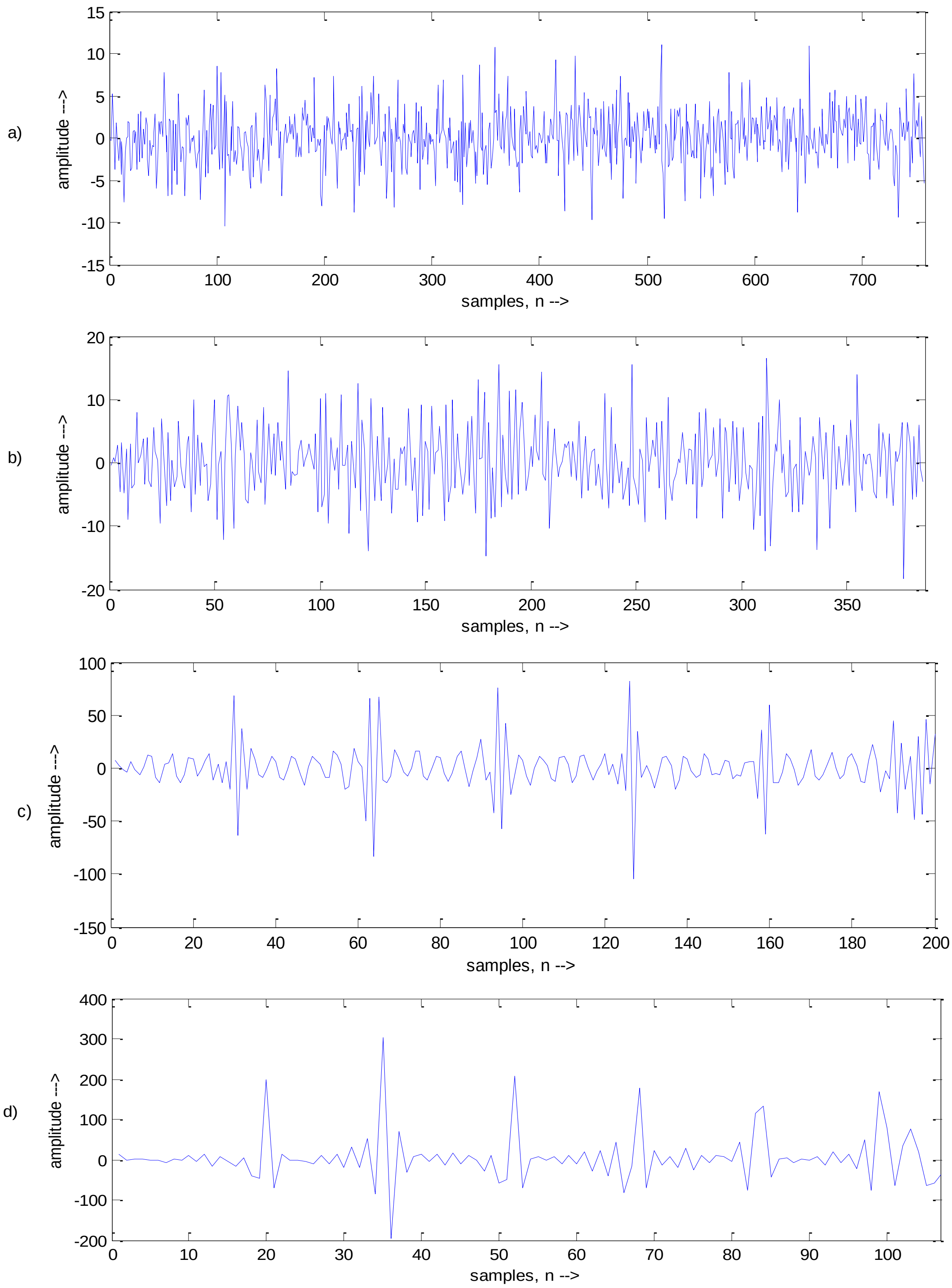

Figure 4.19 Detailed coefficients a) cD_1 : detailed coefficients at level 1, b) cD_2 : detailed coefficients at level 2, c) cD_3 : detailed coefficients at level 3, d) cD_4 : detailed coefficients at level 4

Then the approximate coefficients at level 4 (cA_4) are set to zero. After that, inverse wavelet transform (IDWT) of the modified coefficients are taken to obtain the approximate noise of the ECG signal. The approximated noise signal is shown in Fig. 4.20. The residue of the raw signal and the approximate noise is obtained to get noise free ECG signal. The denoised ECG signal is given in Fig. 4.21.

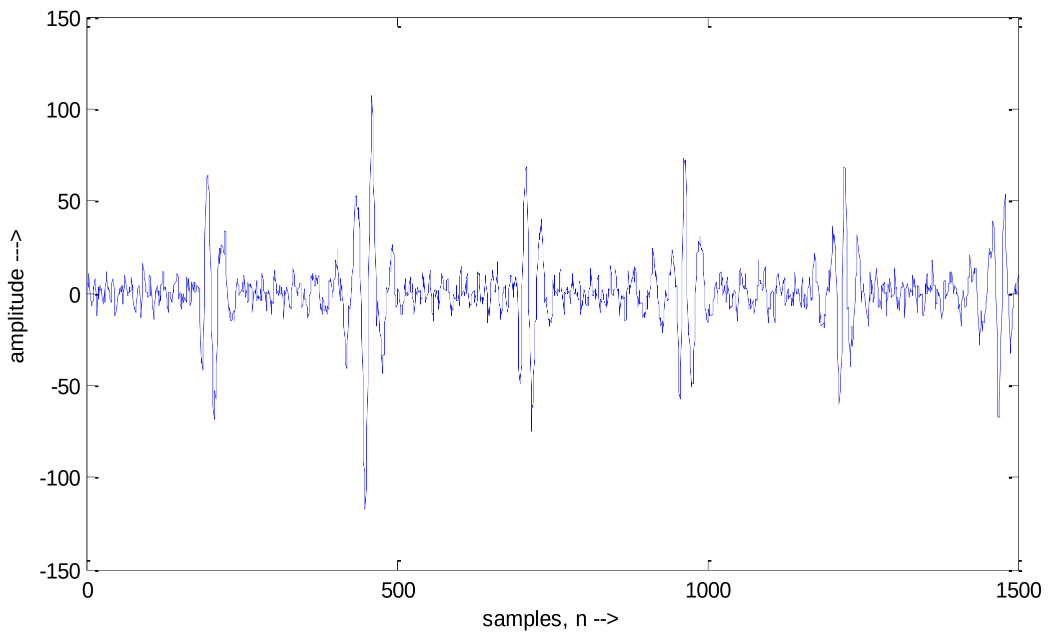

Figure 4.20 Approximated noise

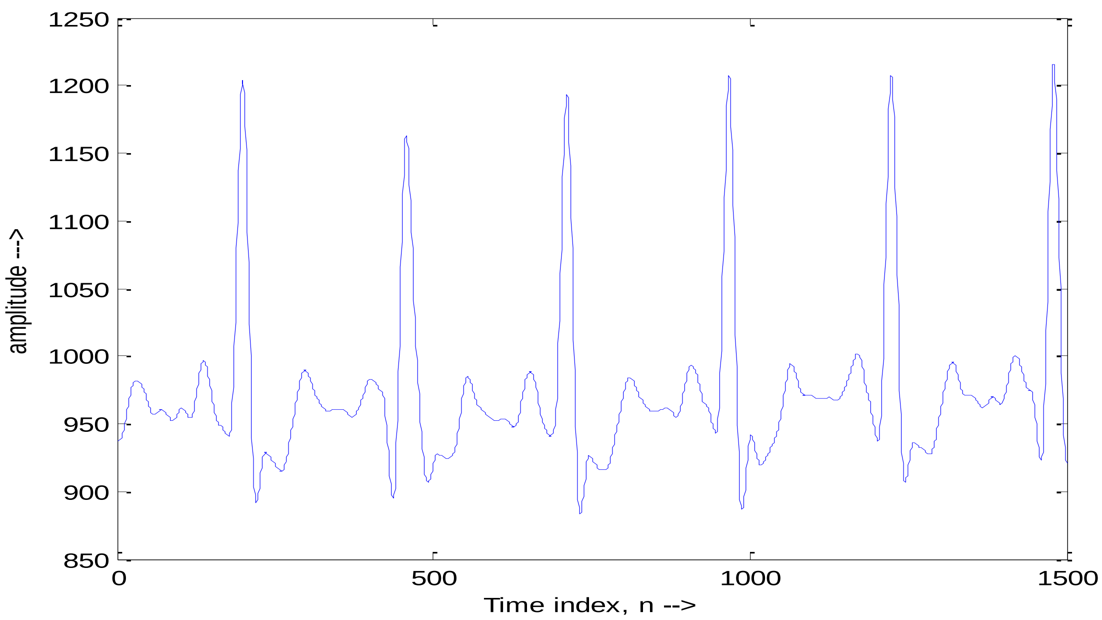

Figure 4.21 Denoised ECG using wavelet filter bank

Chapter 5

Conclusion and Future Scope

This chapter focuses on the advantages and limitations of all the algorithms used for ECG enhancement. The scopes of future research work in this domain are also discussed.

5.1 CONCLUSION

This thesis throws light on the basics of electrocardiogram, artifacts corrupting the ECG signal and ECG enhancement using different algorithms. The thesis begins with the review of some popular work in the field of ECG signal processing. The physiology of heart, heart beat generation, morphology of electrocardiogram are elaborately discussed. Different types of noises that affect the ECG and their origins are also described. For the simulations, the ECG signals are taken from the MIT-BIH data base. The later part of the thesis deals with all the filtering algorithms that are used and the simulation results.

The filtering algorithms used in this thesis are window based FIR filtering, adaptive filtering and wavelet filter bank technique. The advantage and limitations of all the used methods are discussed below.

- The first algorithm is the window based FIR filters, which are designed using Rectangular window, Hamming window, Hanning window and Blackman window. The designed filters are of order 100. The high pass filter has cut-off frequency 3 Hz, the low pass filter of cut-off frequency 100 Hz and the notch filter has notch at 50 Hz. The performance of Rectangular window based filter is better than the rest window based filters as the Rectangular filter has sharp attenuation and pulsation present in the stop band. The phase response of Rectangular window based filter is linear and the filter is also stable.

- The second algorithm analyses the performance of different adaptive filters for ECG denoising. In NLMS based adaptive filter, the step size is greater than LMS algorithm and hence the convergence is faster. NLMS based adaptive filter offers better performance than the LMS counterpart. The computational complexity of NLMS is slightly higher. In all the sign LMS algorithms, the computation is faster because these algorithms does not involve multiplication when error $e(n)$ or input $x(n)$ or both are zero. But the major drawback is that the weight update mechanism is degraded compared to LMS algorithm. Increase in steady state error and decrease in the convergence rate are other minor drawbacks. So, NLMS algorithm is preferred when better performance is required. Sign based adaptive algorithms are chosen when faster performance is needed.

- The third algorithm is wavelet filter bank based denoising, in which the low and high frequency components in the noisy ECG signal *x(n)* is analyzed by passing it through a series of low-pass and high-pass filters with different cut-off frequencies. This is achieved by using scaling function and mother wavelet function. To remove the power line interference and the high frequency noise, the DWT is computed to level 4 using *symlet8* mother wavelet function and scaling function. Then the approximate coefficients at level 4 (cA_4) are set to zero. After that, inverse wavelet transform (IDWT) of the modified coefficients are taken to obtain the approximate noise of the ECG signal. The residue of the raw signal and the approximate noise is obtained to get noise free ECG signal. The proposed method removes noise from the ECG signal without any distortion of the ECG signal features.

5.2 FUTURE SCOPE

In the present work, the window based FIR and LMS algorithm based adaptive filters remove the high frequency, power line interference and low frequency noises. In wavelet filter bank based denoising, only high frequency noise and power line interference are removed. The future developments to this work can be made as follows :

- Implementation of wavelet based denoising for the removal of base line wander.
- Use of other adaptive methods like FT-RLS, QRD-RLS algorithms for ECG denoising.
- Application of blind adaptive filtering for ECG enhancement.
- Real time application of implemented algorithms.

Bibliography

1. R. Acharya, J. S. Suri, J. A.E. Spaan and S .M. Krishnan, “Advances in Cardiac Signal Processing”, 2007 edition, *Springer Berlin Heidelberg, New York* , ISBN: 3-540-36674-1.

2. J. Moss and S. Stern., “Non-invasive electrocardiology: Clinical aspects of holter monitoring”, 1st edition, 1996, *W.B. Saunders, Philadelphia,* ISBN: 9-7020-1925-9.

3. S.K. Jagtap, M.S. Chavan, R.C. Wagvekar and M.D. Uplane, “Application of the digital filter for noise reduction in electrocardiogram”. *Journal of Instrumentation*, vol.40, no. 2, pp. 83–86, June 2010.

4. Dr. K. L. Yadav and Sachin Singh, “Performance evaluation of different adaptive filters for ECG signal processing”, *International Journal On Computer Science and Engineering,* vol. 40, no. 5, pp. 1880–1883, 2010.

5. Muhammad ZiaUrRahman, Rafi Ahamed Shaik and D.V.RamaKoti Reddy, “Efficient sign based normalized adaptive filtering techniques for cancelation of artifacts in ECG signals: Application to wireless biotelemetry”, *Journal of signal processing,* vol. 91, no. 2, pp. 225–239, February 2011.

6. Ching-Haur Chang ,Kang-Ming Chang ,and Hsien-Ju Ko, “Cancellation of highfrequency noise in ECG signals using Adaptive filter without external reference”, *Proceedings of International Conference on Biomedical Engineering and Informatics*, pp. 787–790, Yantai, October 2010.

7. K. Daqrouq, “ECG base line wander reduction using discrete wavelet transform”, *Asian Journal of Information Technology,* vol. 4, no. 11, pp. 989–995, 2005.

8. H.A. Kestler, M.Haschka, W. Kratz, F.Schwenker, G.Palm, V. Hombach, M. Hoher, "De-noising of high-resolution ECG signals by combining the discrete wavelet transform with theWiener filter", *Proceedings of International conference on Computers in Cardiology*, pp. 233–236, Cleveland, OH, September 1998.

9. D. L. Donoho, "De-noising by soft-thresholding", *IEEE Transaction on Information Theory*, vol. 41, no. 3, pp. 613–627, May 1995.

10. M. Popescu, P. Cristea and A. Bezerianos, "High resolution ECG filtering using adaptive BSayesian wavelet shrinkage", *Proceedings of International conference on Computers in Cardiology*, pp. 401–404, Cleveland, OH, September 1998.

11. P.M. Agante, J.P. Marques de Sa, "ECG noise filtering using wavelets with soft-thresholding methods", Proceedings *of International conference on Computers in Cardiology*, pp. 535–538, Hannover, Germany, September 1999.

12. O. Sayadi and M.B. Shamsollahi, "Multi-adaptive bionic wavelet transform: application to ECG denoising and baseline wander reduction", *EURASIP Journal of Applied Signal Processing*, vol. 2007, pp. 1–11, January 2007.

13. Brij N. Singh and Arvind K. Tiwari, "Optimal selection of wavelet basis function applied to ECG signal denoising", *Joiunal of Digital Signal Processing*, vol. 16, no. 3, pp. 275–287, May 2006.

14. G. B. Moody and R. G. Mark, "QRS morphology representation and noise estimation using the Karhunen-Loeve transform", *Proceedings of International conference on Computers in Cardiology*, pp. 269–272, Jerusalem, Israel, September 1989.

15. A. K. Barros, A. Mansour and N. Ohnishi, "Removing artifacts from electrocardiographic signals using independent components analysis", *Journal of Neuro-computing*, vol. 22, no. 1–3, pp. 173–186, 1998.

16. T. He, G. D. Clifford, and L. Tarassenko, "Application of independent component analysis in removing artefacts from the electrocardiogram," *Journal of Neural Computing Applications*, vol. 15, no. 2, pp. 105–116, 2006.

17. G. D. Clifford, L. Tarassenko and N. Townsend, “One-pass training of optimal architecture auto-associative neural network for detecting ectopic beats”, *Electronics letters,* vol. 37, no. 18, pp. 1126-1127, August 2001.

18. Jan Adamec, Richard Adamec, Lukas Kappenberger and Philippe Coumel , ECG Holter : Guide to Electrocardiographic Interpretation,2008 edition, *springer science+business media, LLC, New York*, ISBN-978-0-387-78186-0.

19. Joseph T. Catalano, “Guide to ECG Analysis”, 2nd edition, 2002, *Lippincott Williams & Wilkins, Philadelphia*, ISBN-0-7817-2930-0.

20. http://en.wikipedia.org/wiki/Electrocardiography.

21. Arnold M. Katz, “Physiology of the Heart”, 5th edition, 2011, *Lippincott Williams & Wilkins, Philadelphia*, ISBN 10:1-60831-171-6.

22. Lionel H. Opie, “Heart Physiology: From Cell to Circulation”, 4th edition, 2004, *Lippincott Williams & Wilkins, Philadelphia,* ISBN 13:978-0-7817-4278-8.

23. M. Gabriel Khan , “Rapid ECG Interpretation” , 3rd edition, 2008 , *Humana press, New York*, ISBN- 978-1-58829-979-6.

24. Tomas B. Garcia, Neil E. Holtz, “12 Lead ECG: The Art of Interpretation”, 2001 edition, *Jones & Bartlett publishers, Canada,* ISBN-0-7637-1284-1.

25. Kathryn Monica Lewis and Kathleen A. Handal ,”Sensible Analysis of the 12-Lead ECG”, 2000 edition, *Cengage Learning, Canada* ,ISBN- 0-7668-0524-7.

26. http://www.physionet.org/physiobank/database/mitdb/
MIT-BIH Database distribution, Massachusetts Institute of Technology, 77 Massachusetts Avenue, Cambridge.

27. R.G. Mark, P.S. Schluter, G.B. Moody, P.H. Devlin and D. Chernoff, “An annotated ECG database for evaluating arrhythmia detectors”, *IEEE Transactions on Biomedical Engineering*, vol. 29, no. 8, pp. 600,1982.

28. G.B. Moody and R.G. Mark, "The MIT-BIH Arrhythmia Database on CD-ROM and software for use with it", *Proceedings of International conference on* Computers in Cardiology, pp. 185-188, Chicago, September 1990.

29. Carson K. S. Pun, S. C. Chan, K. S. Yeung, and K. L. Ho, On the design and implementation of FIR and IIR digital filters with variable frequency characteristics, *IEEE transactions on circuits and systems-II: analog and digital signal processing*, vol. 49, no. 11, pp. 689 – 703, November 2002.

30. John G. Proakis and Dimitris G. Manolakis, "Digital signal processing: Principles, algorithms, and applications" , 4th edition, 2007, *Pearson education*, ISBN: 978-81-317-1000-5.

31. N. B. Jones and J. D. McK. Watson, "Digital Signal Processing: Principles, Devices and Applications", 1990 edition, *Peter peregrines Ltd., London, UK*, ISBN: 0-86341-210-6.

32. Emmanuel C. Ifeachor and Barrie W. Jervis, "Digital Signal Processing :A practical approach", 2nd edition, 2009, *pearson education Ltd.*, ISBN: 978-81-317-0824-8.

33. Kangshun Li and Yuan Liu, "The FIR window function design based on evolutionary algorithm", *Proceedings of International Conference on Mechatronic Science, Electric Engineering and Computer (MEC)*, pp. 1797 – 1800, Jilin, China , August 2011.

34. Paulo S.R. Diniz, "Adaptive Filtering Algorithms and Practical Implementation", Springer ,3rd edition, 2008, ISBN 978-0-387-31274-3

35. A.Bhavani Sankar , D.Kumar and K.Seethalakshmi, "Performance Study of Various Adaptive Filter Algorithms for Noise Cancellation in Respiratory Signals", *Signal Processing : An International Journal (SPIJ)*, vol. 4, no. 5, pp. 267-278, December 2010.

36. Hong Wanl, Rongshen Ful and Li Shi, "The Elimination of 50 Hz Power Line Interference from ECG Using a Variable Step Size LMS Adaptive Filtering Algorithm" , *Life Science Journal*, vol. 3, no. 4, 2006

37. D. Z. Chen, Z. Y. Lin, M. Ramahi and R. K. Mittal, "Adaptive cancellation of ECG artifacts in the diaphragm electromyographic signals obtained through intraoesophageal

electrodes during swallowing and inspiration”, *journal of Gastroenterology & Hepatology, wiley,* vol. 6, no. 4, pp. 279-288, June 2008.

38. Y.T. Zhang and R.M. Rangayyan, “Adaptive cancellation of muscle contraction interference in vibroarthrographic signals”, *IEEE Transactions on Biomedical Engineering*, vol. 41, no. 2, pp. 181-191, February 1994

39. V. Almenar and A. Albiol, A new adaptive scheme for ECG enhancement, *Journal of signal processing*, vol. 75, no. 3, pp. 253-263, June 1999

40. Mahmoodabadi and S. Ahmadian, “ECG feature extraction based on multiresolution wavelet transform”, *Proceedings of the IEEE 27th Annual Conference on Engineering in Medicine and Biology*, pp. 3902–3905, Shanghai, China, January 2005.

41. S. Saxena, V. Kumar and S. Hande, “QRS detection using new wavelets”, *Journal of Medical Engineering and Technology*, vol. 26, no. 1, pp. 7–15, 2002

42. Stephane G. Mallat, “A theory for multiresolution signal decomposition: The wavelet representation”, *IEEE Transactions on Pattern Analysis and Machine Intelligence*, Vol. 11 , no. 7, pp. 674–693, August 1989.

43. O. Rioul and M. Vetterli, “Wavelets and signal processing” , *IEEE Signal Processing Magazine*, vol. 8, no. 4, pp. 14–38, August 1991.

44. M. Vettereli, “Wavelets, approximation and compression”, *IEEE Signal Processing Magazine*, vol. 18, no. 5, pp. 59–73, August 2001.

45. I. Daubechies, “The wavelet transform, time-frequency localization and signal analysis”, *IEEE Transanction on Information Theory*, vol. 36, no. 5, pp. 961–1005, 1990.

Dissemination

Journal:

1. Rashmi Panda, Umesh C. pati, "Performance analysis of LMS based adaptive filter algorithms for ECG denoising" , **Accepted** for publication in *Journal of Instrument Society of India*, June 2012.

Conference:

1. Rashmi Panda, Umesh C. pati, “Removal of artifacts from electrocardiogram using digital filter”, *Proceedings of IEEE Students’ Conference on Electrical, Electronics and Computer Science*, pp. 1-4, Bhopal, March 2012 (**Published**)